

# A variational form of the equivalent inclusion method for numerical homogenization

Sébastien Brisard, Luc Dormieux, Karam Sab

► **To cite this version:**

Sébastien Brisard, Luc Dormieux, Karam Sab. A variational form of the equivalent inclusion method for numerical homogenization. *International Journal of Solids and Structures*, Elsevier, 2014, 51 (3-4), pp.716-728. 10.1016/j.ijsolstr.2013.10.037 . hal-00922779

**HAL Id: hal-00922779**

**<https://hal-enpc.archives-ouvertes.fr/hal-00922779>**

Submitted on 30 Dec 2013

**HAL** is a multi-disciplinary open access archive for the deposit and dissemination of scientific research documents, whether they are published or not. The documents may come from teaching and research institutions in France or abroad, or from public or private research centers.

L'archive ouverte pluridisciplinaire **HAL**, est destinée au dépôt et à la diffusion de documents scientifiques de niveau recherche, publiés ou non, émanant des établissements d'enseignement et de recherche français ou étrangers, des laboratoires publics ou privés.

# A variational form of the equivalent inclusion method for numerical homogenization

S. Brisard<sup>a,\*</sup>, L. Dormieux<sup>a</sup>, K. Sab<sup>a</sup>

<sup>a</sup>Université Paris-Est, Laboratoire Navier (UMR 8205), CNRS, ENPC, IFSTTAR, F-77455 Marne-la-Vallée

---

## Abstract

Due to its relatively low computational cost, the equivalent inclusion method is an attractive alternative to traditional full-field computations of heterogeneous materials formed of simple inhomogeneities (spherical, ellipsoidal) embedded in a homogeneous matrix. The method can be seen as the discretization of the Lippmann–Schwinger equation with piecewise polynomials. Contrary to the original approach of Moschovidis and Mura, who discretized the strong form of the Lippmann–Schwinger equation through Taylor expansions, we propose in the present paper a Galerkin discretization of the weak form of this equation. Combined with the new, mixed boundary conditions recently introduced by the authors, the resulting method is particularly well-suited to homogenization. It is shown that this new, variational approach has a number of benefits: (i) the resulting linear system is well-posed, (ii) the numerical solution converges to the exact solution as the maximum degree of the polynomials tends to infinity and (iii) the method can provide rigorous bounds on the apparent properties of the statistical volume element, provided that the matrix is stiffer (or softer) than all inhomogeneities. This paper presents the formulation and implementation of the new, variational form of the equivalent inclusion method. Its efficiency is investigated through numerical applications in 2D and 3D elasticity.

NOTICE: this is the author's version of a work that was accepted for publication in the *International Journal of Solids and Structures*. Changes resulting from the publishing process, such as peer review, editing, corrections, structural formatting, and other quality control mechanisms may not be reflected in this document. Changes may have been made to this work since it was submitted for publication. A definitive version was subsequently published in the *International Journal of Solids and Structures* **51(3-4)**, pp. 716–728, 2014 (<http://dx.doi.org/10.1016/j.ijsolstr.2013.10.037>).

**Keywords:** Homogenization, Elasticity, Equivalent Inclusion Method, Galerkin Discretization, Green Operator

---

## 1. Introduction

A wide range of tools are available for the determination of the macroscopic properties of heterogeneous materials. Standard micromechanical techniques, based on the solution of Eshelby (1957), are found at one end of this range. Examples of such techniques are the scheme Mori and Tanaka (1973) [see also Benveniste (1987)] and the self-consistent scheme (Walpole, 1969; Kröner, 1977). Although not based on the solution of Eshelby (1957), the generalized self-consistent scheme (Christensen and Lo, 1979; Hervé and Zaoui, 1993) also falls into this category. The main asset of these schemes is their flexibility, as they apply to linear as well as non-linear behaviours (Suquet, 1997), while leading to analytical or semi-analytical models; various types of couplings can also be included. The weakness of such models lies in the limited amount of microstructural information they can account for in a quantitative way: volume fractions and possibly distributions of orientations, but no higher-order correlations.

Full-field calculations can be found at the other end of this range. These computation return the ‘exact’ (up to some numeri-

cal error) local strains and stresses of a specific realization of the material. Standard (finite elements, boundary elements) as well as non-standard [based for example on the Fast Fourier Transform (Moulinec and Suquet, 1998)] homogenization techniques can be used for this computation. Contrary to the micromechanical technique, the amount of microstructural information that full-field calculations can account for is limited by the resolution (or fineness of the mesh) only, thus leading to models with greater accuracy. However, such type of computations are also much more demanding both in terms of memory and processing time, to the effect that advanced techniques such as parallelization or multi-threading are usually invoked. This can be problematic for stastical analyses requiring computations on numerous microstructures (Kanit et al., 2003; Ostoja-Starzewski, 2006).

The equivalent inclusion method is an intermediate technique which is both more accurate than micromechanical approaches, and less costly than full-field computations. Like the latter, it requires a realization of the material under investigation, and produces estimates of the local strain and stress fields. Because the total number of degrees of freedom remains limited, the required memory and processing time are lowered. It should also be noted that the preparation of the computation is straightforward, as no mesh of the microstructure is required. The price

---

\*Corresponding author.

Email addresses: [sebastien.brisard@ifsttar.fr](mailto:sebastien.brisard@ifsttar.fr) (S. Brisard), [luc.dormieux@enpc.fr](mailto:luc.dormieux@enpc.fr) (L. Dormieux), [karam.sab@enpc.fr](mailto:karam.sab@enpc.fr) (K. Sab)

to pay is, of course, a loss of accuracy with respect to full-field computations. Still, the accuracy gain over micromechanical approaches can be significant.

The equivalent inclusion method finds its roots in the pioneering work of Eshelby (1957), who derived the exact solution to the problem of a single ellipsoidal inhomogeneity, embedded in an infinite matrix. To this end, he introduced a strictly equivalent ellipsoidal inclusion, with appropriate eigenstrain. Moschovidis and Mura (1975) then extended this work to find an approximate solution to the problem of multiple inhomogeneities, embedded in an infinite matrix. Similarly, each inhomogeneity is substituted with an inclusion, which is equivalent only in an approximate sense. The eigenstrains to which the inclusions are submitted are found by solving a linear system, resulting from a discretization of the so-called consistency equation by means of Taylor expansions. Since this consistency equation is equivalent to the Lippmann–Schwinger equation (Korringa, 1973; Zeller and Dederichs, 1973; Kröner, 1974), the equivalent inclusion method can be seen as a particular discretization of this integral equation.

Although many applications of the equivalent inclusion method found in the literature deal with pairs of inhomogeneities (Moschovidis and Mura, 1975; Rodin and Hwang, 1991; Shodja et al., 2003), some authors have successfully applied this technique to problems involving many inclusions (Fond et al., 2002; Benedikt et al., 2006). It has also recently been used to enrich the shape functions of finite element models with non-conforming meshes (Novák et al., 2012).

The equivalent inclusion method is limited to composites with ellipsoidal inhomogeneities and homogeneous matrix. While this might be too stringent a restriction for many real materials, this method is a valuable tool for the quantification –on model microstructures– of the influence of some specific microstructural parameters, such as particle-size distribution, or local orientational order.

In this paper, a variational form of the equivalent inclusion method is introduced. It is based on a Galerkin discretization (through piecewise polynomials) of a modified Lippmann–Schwinger equation, which is better-suited to numerical homogenization than the standard Lippmann–Schwinger equation (Brisard et al., 2013b). The new, variational form of the equivalent inclusion method improves upon its original, Taylor-based form in many respects. Indeed, the resulting linear system is well-posed, and convergence with respect to the degree of the polynomial approximations can be proved. By contrast, none of these results has been established for the Taylor-based equivalent inclusion method, and examples can be found where increasing the degree of the polynomials actually lowers the accuracy of the approximations (Fond et al., 2001). Furthermore, the principle of Hashin and Shtrikman (1962a), extended to the modified Lippmann–Schwinger equation (Brisard et al., 2013b), can be used to show that the Galerkin-based equivalent inclusion method provides rigorous bounds on the macroscopic properties.

The present paper is organized as follows. Sec. 2 provides some background information regarding the original (Taylor-based) equivalent inclusion method and its relation to the Lippmann–Schwinger equation, as well as its application to numerical ho-

mogenization. Sec. 3 introduces the variational framework for the proposed alternative version of the equivalent inclusion method. The discretized equations are derived from a Galerkin approach. Using the principle of Hashin and Shtrikman (1962a) [see also Hill (1963b) and Willis (1977)], it is then shown that the newly introduced method can provide bounds on the macroscopic properties. Sec. 4 provides technical details on the implementation of the method. In particular, the calculation of the self-influence and influence pseudotensors is presented. Finally, some applications are proposed in Sec. 5 to illustrate the efficiency of the method.

In the remainder of this paper, we refer to the original (Taylor-based) form of the equivalent inclusion method as EIM-T. Likewise, EIM-G refers to the new (Galerkin-based) form of the equivalent inclusion method.

## 2. Background

The present section provides background information on the equivalent inclusion method and its application to numerical homogenization. The presentation below differs from the original paper by Moschovidis and Mura (1975), in that the Green operator for strains  $\Gamma_0^\infty$  is used in place of the potentials  $\Phi_{ij}$  and  $\Psi_{ij}$ . Furthermore, derivation of the EIM-T is traditionally based on eigenstrains (Moschovidis and Mura, 1975). By contrast, the EIM-G presented in this paper is most conveniently derived using prestresses (more precisely, polarizations). As a consequence, slightly altering the terminology introduced by Eshelby (1957), an inclusion is defined in the present paper as a region in a homogeneous medium (no material mismatch), subjected to eigenstrains *or* prestresses. By contrast, an inhomogeneity is a region in a heterogeneous medium which is occupied by a homogeneous material whose mechanical properties differ from those of the matrix.

Sec. 2 is organized as follows. In Sec. 2.1, the tuple notation is first introduced, which will allow for more compact formulas in the remainder of this paper. Then, in Sec. 2.2, the fundamentals of the equivalent inclusion (EIM-T) method are briefly recalled. Following Moschovidis and Mura (1975), the derivation of the method is based on eigenstrains; unlike these authors, our formulation of the consistency equation makes explicit use of the Green operator for strains. This reveals important connections between the EIM-T and the well-known Lippmann–Schwinger equation (Korringa, 1973; Zeller and Dederichs, 1973; Kröner, 1974). Finally, applicability of this method to numerical homogenization is discussed in Sec. 2.3.

### 2.1. On the tuple notation

In the remainder of this paper, quantities indexed with a dot (e.g.  $k_\bullet, l_\bullet, x_\bullet, y_\bullet, \dots$ ) denote  $d$ -tuples; in particular,  $0_\bullet$  denotes the null tuple

$$0_\bullet = \underbrace{(0, \dots, 0)}_{d \text{ times}}.$$

Depending on the context, the components of the tuple can be naturals or reals. For example,  $k_\bullet = (k_i)_{1 \leq i \leq d} \in \mathbb{N}^d$  denotes a

multi-index, while  $x_{\bullet} = (x_i)_{1 \leq i \leq d} \in \mathbb{R}^d$  denotes the coordinates of the vector  $\mathbf{x}$  with respect to the global basis  $(\mathbf{e}_i)_{1 \leq i \leq d}$ . Similarly,  $x'_{\bullet} = (x'_j)_{1 \leq j \leq d} \in \mathbb{R}^d$  denotes the coordinates of  $\mathbf{x}$  with respect to an auxiliary basis  $(\mathbf{e}'_j)_{1 \leq j \leq d}$ .

For any tuple  $a_{\bullet}$ ,  $a_+$  (resp.  $a_{\times}$ ) denotes the sum (resp. product) of its components

$$a_+ = a_1 + \dots + a_d, \text{ and } a_{\times} = a_1 \dots a_d.$$

In particular,  $dx_{\times}$  is the following volume element

$$dx_{\times} = dx_1 \dots dx_d.$$

It is understood that all binary operators  $(+, \times, \leq, \dots)$  should apply component-wise to tuples. For example,

$$a_{\bullet} + b_{\bullet} = c_{\bullet}, \text{ where } c_i = a_i + b_i \text{ for all } i = 1, \dots, d,$$

similarly

$$a_{\bullet} \leq b_{\bullet} \text{ if, and only if, } a_i \leq b_i \text{ for all } i = 1, \dots, d.$$

Exponentiation of tuples is then defined as follows

$$x_{\bullet}^{n_{\bullet}} = x_1^{n_1} \dots x_d^{n_d},$$

and it should be noted that the above quantity is not intrinsic, as it depends on the components  $x_1, \dots, x_d$  of the vector  $\mathbf{x}$  in a specified basis. In particular,  $\mathbf{x}^{n_{\bullet}}$  would not be a meaningful notation, since  $x_{\bullet}^{m_{\bullet}} \neq x_{\bullet}^{n_{\bullet}}$ . From the binomial theorem

$$(a_{\bullet} + b_{\bullet})^{n_{\bullet}} = \sum_{0_{\bullet} \leq l_{\bullet} \leq n_{\bullet}} \binom{n_{\bullet}}{l_{\bullet}} a_{\bullet}^{l_{\bullet}} b_{\bullet}^{n_{\bullet} - l_{\bullet}}, \quad (1)$$

where the following multi-binomial coefficient has been defined

$$\binom{n_{\bullet}}{l_{\bullet}} = \binom{n_1}{k_1} \dots \binom{n_d}{k_d} = \frac{n_1!}{k_1! (n_1 - k_1)!} \dots \frac{n_d!}{k_d! (n_d - k_d)!}.$$

## 2.2. The equivalent inclusion method

*The N-inhomogeneity problem.* The equivalent inclusion method allows the computation of the approximate strain field in an assembly of inhomogeneities, embedded in an infinite matrix, and submitted to a uniform strain at infinity.

The microstructure under consideration is formed of  $N$  inhomogeneities  $\Omega_1, \dots, \Omega_N \subset \mathbb{R}^d$  ( $d$ : dimension of the physical space), embedded in an infinite matrix  $\Omega_0 = \mathbb{R}^d \setminus (\Omega_1 \cup \dots \cup \Omega_N)$ . Inhomogeneity  $\alpha$  is centered at  $\mathbf{x}_{\alpha}$  ( $\alpha = 1, \dots, N$ ), and  $\chi_{\alpha}$  denotes the indicator function of inhomogeneity  $\alpha$ , translated back to the origin. In other words,  $\mathbf{x} \in \Omega_{\alpha}$  if, and only if,  $\chi_{\alpha}(\mathbf{x} - \mathbf{x}_{\alpha}) = 1$ ; besides,  $\chi_{\alpha} = \chi_{\beta}$  if inhomogeneities  $\alpha$  and  $\beta$  are identical (up to a translation).

Assuming a linear elastic behaviour for all constituents,  $\mathbf{C}_{\alpha}$  (resp.  $\mathbf{C}_0$ ) denotes the elastic stiffness of inhomogeneity  $\alpha$  (resp. the matrix). The local stiffness, defined over the whole space  $\mathbb{R}^d$  then reads

$$\mathbf{C}(\mathbf{x}) = \mathbf{C}_0 + \sum_{\alpha=1}^N \chi_{\alpha}(\mathbf{x} - \mathbf{x}_{\alpha}) (\mathbf{C}_{\alpha} - \mathbf{C}_0). \quad (2)$$

With this notation at hand, the problem to be solved by the equivalent inclusion method reads (Fig. 1, left)

$$\nabla_{\mathbf{x}} \cdot \boldsymbol{\sigma} = \mathbf{0} \quad (\mathbf{x} \in \mathbb{R}^d), \quad (3a)$$

$$\boldsymbol{\sigma}(\mathbf{x}) = \mathbf{C}(\mathbf{x}) : \boldsymbol{\varepsilon}(\mathbf{x}) \quad (\mathbf{x} \in \mathbb{R}^d), \quad (3b)$$

$$\boldsymbol{\varepsilon}(\mathbf{x}) = \nabla_{\mathbf{x}}^s \mathbf{u} \quad (\mathbf{x} \in \mathbb{R}^d), \quad (3c)$$

$$\mathbf{u}(\mathbf{x}) \sim \mathbf{E}^{\infty} \cdot \mathbf{x} \quad (\|\mathbf{x}\| \rightarrow +\infty), \quad (3d)$$

under the constraint that  $\boldsymbol{\varepsilon} - \mathbf{E}^{\infty}$  be square-integrable to ensure well-posedness (Brisard et al., 2013b). In Eqs. (3),  $\mathbf{u}$  (resp.  $\boldsymbol{\varepsilon}$ ,  $\boldsymbol{\sigma}$ ) denotes the local displacement (resp. strain, stress); furthermore,  $\nabla^s \mathbf{u}$  denotes the symmetric gradient of the displacement. Boundary conditions (3d) will be called KUBC $^{\infty}$  [Kinematic Uniform Boundary Conditions at infinity, see Brisard et al. (2013b)].

*The N-inclusion problem.* Prior to solving problem (3), Moschovidis and Mura (1975) consider the following auxiliary  $N$ -inclusion problem, in which  $\Omega_1, \dots, \Omega_N$  are inclusions rather than inhomogeneities, submitted to the uniform strain at infinity  $\mathbf{E}^{\infty}$  and the eigenstrain  $\boldsymbol{\eta}$  (Fig. 1, right)

$$\nabla_{\mathbf{x}} \cdot \boldsymbol{\sigma} = \mathbf{0} \quad (\mathbf{x} \in \mathbb{R}^d), \quad (4a)$$

$$\boldsymbol{\sigma}(\mathbf{x}) = \mathbf{C}_0 : (\boldsymbol{\varepsilon}(\mathbf{x}) - \boldsymbol{\eta}(\mathbf{x})) \quad (\mathbf{x} \in \mathbb{R}^d), \quad (4b)$$

$$\boldsymbol{\varepsilon}(\mathbf{x}) = \nabla_{\mathbf{x}}^s \mathbf{u} \quad (\mathbf{x} \in \mathbb{R}^d), \quad (4c)$$

$$\mathbf{u}(\mathbf{x}) \sim \mathbf{E}^{\infty} \cdot \mathbf{x} \quad (\|\mathbf{x}\| \rightarrow +\infty). \quad (4d)$$

It should be noted that  $\boldsymbol{\eta}(\mathbf{x}) = \mathbf{0}$  for all  $\mathbf{x} \in \Omega_0$ ; besides, contrary to the single-inclusion problem of Eshelby (1957), the eigenstrain  $\boldsymbol{\eta}$  is allowed to vary spatially within each inclusion. The solution to the  $N$ -inclusion problem (4) depends linearly on  $\mathbf{E}^{\infty}$  and  $\boldsymbol{\eta}$ . It is conveniently written in terms of the Green operator for strains  $\Gamma_0^{\infty}$  of the homogeneous, infinite medium  $\mathbf{C}_0$ . It is recalled that this operator returns the opposite of the strain induced in the reference, unbounded medium by any prestress  $\boldsymbol{\varpi}$  (Korringa, 1973; Zeller and Dederichs, 1973; Kröner, 1974). In other words

$$\Gamma_0^{\infty} * \boldsymbol{\varpi} = -\nabla^s \mathbf{u}, \quad (5)$$

where  $*$  stands for the standard convolution product, and  $\mathbf{u}$  is the solution to the following partial differential equation in  $\mathbb{R}^d$

$$\nabla \cdot (\mathbf{C}_0 : \nabla^s \mathbf{u} + \boldsymbol{\varpi}) = \mathbf{0}, \quad (6)$$

with  $\nabla^s \mathbf{u}$  square integrable and  $\mathbf{u}(\mathbf{x}) \rightarrow \mathbf{0}$  as  $\|\mathbf{x}\| \rightarrow +\infty$ . From Eqs. (5) and (6), it is readily found that the local strain  $\boldsymbol{\varepsilon}$  solution to the  $N$ -inclusion problem (4) is given by the convolution product

$$\boldsymbol{\varepsilon} = \mathbf{E}^{\infty} + \Gamma_0^{\infty} * (\mathbf{C}_0 : \boldsymbol{\eta}). \quad (7)$$

*From inhomogeneities to inclusions.* To solve the  $N$ -inhomogeneity problem (3), Moschovidis and Mura (1975) proceed in two steps. As a first step, they introduce an equivalent  $N$ -inclusion problem [see Eqs. (8) below]. Equating the elastic stress induced in the homogeneous medium by  $\mathbf{E}^{\infty}$  and  $\boldsymbol{\eta}$  to the

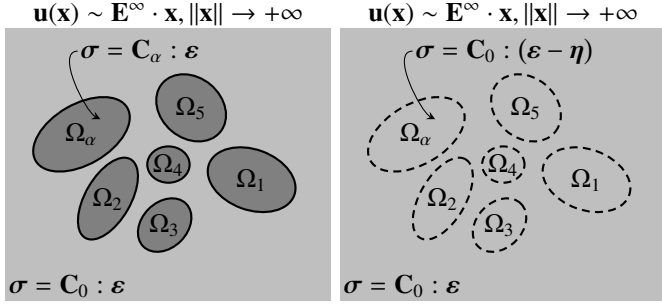


Figure 1: Left: the  $N$ -inhomogeneity problem. Right: the  $N$ -inclusion problem.

stress induced in the heterogeneous medium by  $\mathbf{E}^\infty$  and the material mismatch, they derive the so-called consistency equation, with the eigenstrain  $\boldsymbol{\eta}$  as unknown. As a second step, they then propose a procedure to discretize the consistency equation, thus allowing the numerical computation of approximate solutions to the  $N$ -inhomogeneity problem (3). These two steps are briefly summarized below.

An equivalent formulation of the  $N$ -inhomogeneity problem (3) is first introduced

$$\nabla_{\mathbf{x}} \cdot \boldsymbol{\sigma} = \mathbf{0} \quad (\mathbf{x} \in \mathbb{R}^d), \quad (8a)$$

$$\boldsymbol{\sigma}(\mathbf{x}) = \mathbf{C}_0 : (\boldsymbol{\varepsilon}(\mathbf{x}) - \boldsymbol{\eta}(\mathbf{x})) \quad (\mathbf{x} \in \mathbb{R}^d), \quad (8b)$$

$$\boldsymbol{\eta}(\mathbf{x}) = -\mathbf{C}_0^{-1} : (\mathbf{C}(\mathbf{x}) - \mathbf{C}_0) : \boldsymbol{\varepsilon}(\mathbf{x}) \quad (\mathbf{x} \in \mathbb{R}^d), \quad (8c)$$

$$\boldsymbol{\varepsilon}(\mathbf{x}) = \nabla_{\mathbf{x}}^s \mathbf{u} \quad (\mathbf{x} \in \mathbb{R}^d), \quad (8d)$$

$$\mathbf{u}(\mathbf{x}) \sim \mathbf{E}^\infty \cdot \mathbf{x} \quad (\|\mathbf{x}\| \rightarrow +\infty), \quad (8e)$$

where the quantity  $\boldsymbol{\eta}$  [defined by Eq. (8c)] can be viewed as an eigenstrain applied to  $\Omega_1, \dots, \Omega_N$ , which are no longer inhomogeneities, but inclusions. It should be noted that the eigenstrain  $\boldsymbol{\eta}$  does not affect the matrix  $\Omega_0$  since by construction,  $\boldsymbol{\eta}(\mathbf{x}) = \mathbf{0}$  for  $\mathbf{x} \in \Omega_0$  [see Eq. (8c)]. The solution to Eqs. (8a), (8b), (8d), (8e) is given by Eq. (7), which, upon substitution in Eq. (8c), leads to the so-called consistency equation (Moschovidis and Mura, 1975)

$$(\mathbf{C} - \mathbf{C}_0)^{-1} : \mathbf{C}_0 : \boldsymbol{\eta} = -\mathbf{E}^\infty - \boldsymbol{\Gamma}_0^\infty * (\mathbf{C}_0 : \boldsymbol{\eta}). \quad (9)$$

The consistency equation is an integral equation with the local eigenstrain  $\boldsymbol{\eta}$  as unknown. Its discretization is addressed in the next paragraph. It should be noted that if the local strain  $\boldsymbol{\varepsilon}$  is chosen as main unknown, Eq. (9) reduces to

$$\boldsymbol{\varepsilon} + \boldsymbol{\Gamma}_0^\infty * ((\mathbf{C} - \mathbf{C}_0) : \boldsymbol{\varepsilon}) = \mathbf{E}^\infty,$$

which is known as the Lippmann–Schwinger equation (Korringa, 1973; Zeller and Dederichs, 1973; Kröner, 1974).

Finally, it will be seen in Sec. 3 that the most natural choice of main unknown for the derivation of the EIM-G is neither the local eigenstrain  $\boldsymbol{\eta}$ , nor the local strain  $\boldsymbol{\varepsilon}$ , but the local *polarization*  $\boldsymbol{\tau}$ , defined as follows [see Willis (1977) among others]

$$\boldsymbol{\tau} = (\mathbf{C} - \mathbf{C}_0) : \boldsymbol{\varepsilon} = -\mathbf{C}_0 : \boldsymbol{\eta}. \quad (10)$$

It is readily observed that  $\boldsymbol{\tau}$  is homogeneous to a prestress, and that  $\boldsymbol{\tau}(\mathbf{x}) = \mathbf{0}$  for all  $\mathbf{x} \in \Omega_0$ . With  $\boldsymbol{\tau}$  as main unknown, Eq. (9) reads

$$(\mathbf{C} - \mathbf{C}_0)^{-1} : \boldsymbol{\tau} + \boldsymbol{\Gamma}_0^\infty * \boldsymbol{\tau} = \mathbf{E}^\infty. \quad (11)$$

*Discretization of the consistency equation.* Following Moschovidis and Mura (1975), an approximate solution to Eq. (9) is found by use of piecewise polynomial expansions of degree  $p$  for the eigenstrain  $\boldsymbol{\eta}$

$$\boldsymbol{\eta}(\mathbf{x}) = \sum_{\alpha=1}^N \sum_{\mathbf{k}_\bullet \in \mathfrak{S}^p} \chi_\alpha(\mathbf{x} - \mathbf{x}_\alpha) (x_\bullet - x_{\alpha,\bullet})^{\mathbf{k}_\bullet} \boldsymbol{\eta}_\alpha^{\mathbf{k}_\bullet}, \quad (12)$$

for all  $\mathbf{x} \in \mathbb{R}^d$ , where  $\mathfrak{S}^p$  is the following set of multi-indices  $\mathbf{k}_\bullet$

$$\mathfrak{S}^p = \{\mathbf{k}_\bullet \in \mathbb{N}^d, k_+ \leq p\}.$$

For  $\alpha = 1, \dots, N$  and  $\mathbf{k}_\bullet \in \mathfrak{S}^p$ ,  $\boldsymbol{\eta}_\alpha^{\mathbf{k}_\bullet}$  is a set of  $d^2$  constants  $\eta_{\alpha,ij}^{\mathbf{k}_\bullet}$ , such that  $\eta_{\alpha,ij}^{\mathbf{k}_\bullet} = \eta_{\alpha,ji}^{\mathbf{k}_\bullet}$  ( $i, j = 1, \dots, d$ ); however,  $\boldsymbol{\eta}_\alpha^{\mathbf{k}_\bullet}$  should not be considered as a true second-rank, symmetric tensor. Indeed, Eq. (12) is not intrinsic (because exponentiation is not an intrinsic operation). In particular,  $\boldsymbol{\eta}_\alpha^{\mathbf{k}_\bullet}$  does not follow the required transformation laws under a change of basis. Such objects will be called *pseudotensors* in the remainder of this paper.

Substituting the assumed form (12) for  $\boldsymbol{\eta}$  into Eq. (7), it is readily seen that the local strain  $\boldsymbol{\varepsilon}$  resulting from the imposed uniform strain at infinity  $\mathbf{E}^\infty$  and the piecewise polynomial eigenstrain  $\boldsymbol{\eta}$  defined by Eq. (12) reads

$$\boldsymbol{\varepsilon}(\mathbf{x}) = \mathbf{E}^\infty + \sum_{\beta=1}^N \sum_{\mathbf{l}_\bullet \in \mathfrak{S}^p} \mathbf{D}_\beta^{\mathbf{l}_\bullet}(\mathbf{x} - \mathbf{x}_\beta) : \boldsymbol{\eta}_\beta^{\mathbf{l}_\bullet}, \quad (13)$$

where the fourth-rank pseudotensor  $\mathbf{D}_\beta^{\mathbf{l}_\bullet}$  is defined as follows

$$\mathbf{D}_\beta^{\mathbf{l}_\bullet}(\mathbf{x}) = \int_{\mathbf{y} \in \mathbb{R}^d} \chi_\beta(\mathbf{y}) \mathbf{y}^{\mathbf{l}_\bullet} : \boldsymbol{\Gamma}_0^\infty(\mathbf{x} - \mathbf{y}) : \mathbf{C}_0 dV_{\mathbf{y}}. \quad (14)$$

In the above expression,  $dV_{\mathbf{y}}$  denotes the  $d$ -dimensional volume element at  $\mathbf{y} \in \mathbb{R}^d$ .  $\mathbf{D}_\beta^{\mathbf{l}_\bullet}(\mathbf{x})$  depends on the shape of inclusion  $\beta$ , but not on its position in space; for ellipsoidal inclusions, these pseudotensors can be calculated explicitly [see Moschovidis and Mura (1975) and references therein].

Substitution of Eq. (14) into Eq. (9) leads to the following set of equations which must hold for all  $\alpha = 1, \dots, N$  and  $\mathbf{x} \in \Omega_\alpha$

$$(\mathbf{C}_\alpha - \mathbf{C}_0)^{-1} : \mathbf{C}_0 : \boldsymbol{\eta}(\mathbf{x}) = -\mathbf{E}^\infty - \sum_{\beta=1}^N \sum_{\mathbf{l}_\bullet \in \mathfrak{S}^p} \mathbf{D}_\beta^{\mathbf{l}_\bullet}(\mathbf{x} - \mathbf{x}_\beta) : \boldsymbol{\eta}_\beta^{\mathbf{l}_\bullet}. \quad (15)$$

Clearly, these equations can only be solved for the  $\boldsymbol{\eta}_\beta^{\mathbf{l}_\bullet}$  in an approximate sense. Indeed, the left-hand side of Eq. (15) is polynomial over  $\Omega_\alpha$ , while the right-hand side is not. Following Moschovidis and Mura (1975), it is natural (since the left-hand side is polynomial) to approximate the right-hand side of Eq.

(15) with a Taylor expansion in the neighborhood of the center  $\mathbf{x}_\alpha$  of  $\Omega_\alpha$

$$\mathbf{D}_\beta^{k_\bullet}(\mathbf{x} - \mathbf{x}_\beta) \approx \sum_{k_\bullet \in \mathfrak{S}^p} (x_\bullet - x_{\alpha,\bullet})^{k_\bullet} \mathbf{D}_{\alpha\beta}^{k_\bullet} : \boldsymbol{\eta}_\beta^l, \quad (16)$$

where

$$\mathbf{D}_{\alpha\beta}^{k_\bullet} = \frac{1}{k_1! \cdots k_d!} \left. \frac{\partial^{k_1} \cdots \partial^{k_d} \mathbf{D}_\beta^l}{\partial x_1^{k_1} \cdots \partial x_d^{k_d}} \right|_{\mathbf{x}_\alpha - \mathbf{x}_\beta},$$

and, upon substitution into Eq. (15)

$$\begin{aligned} & \sum_{k_\bullet \in \mathfrak{S}^p} (x_\bullet - x_{\alpha,\bullet})^{k_\bullet} (\mathbf{C}_\alpha - \mathbf{C}_0)^{-1} : \mathbf{C}_0 : \boldsymbol{\eta}_\alpha^{k_\bullet} \\ &= -\mathbf{E}^\infty - \sum_{\beta=1}^N \sum_{k_\bullet, l_\bullet \in \mathfrak{S}^p} (x_\bullet - x_{\alpha,\bullet})^{k_\bullet} \mathbf{D}_{\alpha\beta}^{k_\bullet} : \boldsymbol{\eta}_\beta^{l_\bullet}. \end{aligned}$$

The above identity must be satisfied for all  $\mathbf{x} \in \Omega_\alpha$ . Equating all monomials results in the following set of algebraic equations with unknowns  $\boldsymbol{\eta}_\alpha^{k_\bullet}$  ( $\alpha = 1, \dots, N, k_\bullet \in \mathfrak{S}^p$ )

$$\begin{aligned} (\mathbf{C}_\alpha - \mathbf{C}_0)^{-1} : \mathbf{C}_0 : \boldsymbol{\eta}_\alpha^{k_\bullet} + \sum_{\beta=1}^N \sum_{l_\bullet \in \mathfrak{S}^p} \mathbf{D}_{\alpha\beta}^{k_\bullet} : \boldsymbol{\eta}_\beta^{l_\bullet} \\ = \begin{cases} -\mathbf{E}^\infty & \text{if } k_\bullet = \mathbf{0}_\bullet, \\ \mathbf{0} & \text{otherwise.} \end{cases} \quad (17) \end{aligned}$$

The system of equations (17) defines the original form of the equivalent inclusion method (EIM-T), first derived by Moschovidis and Mura (1975). From the solution to these equations, an approximate expression of the local strain  $\boldsymbol{\varepsilon}(\mathbf{x})$ , solution to the  $N$ -inhomogeneity problem (3) can be computed by means of Eq. (13).

Since the seminal paper of Moschovidis and Mura (1975), alternative linear systems of equations have been proposed. Instead of the inclusions centers  $\mathbf{x}_\alpha$ , Benedikt et al. (2006) compute Taylor expansions of  $\mathbf{D}_\beta^{k_\bullet}$  [see Eq. (16)] at selected points of interest (where the stresses are sought); they show that the resulting estimates are more accurate. However, this approach requires a new inversion of the linear system (17) if a new set of points of interest is considered. Shodja et al. (2003) use point collocation in place of Taylor expansions, which makes the assembly of the linear system much simpler.

Closed-form expressions of the pseudotensors  $\mathbf{D}_{\alpha\beta}^{k_\bullet}$  are available (Mura, 1987); alternatively, they can be computed numerically (Nakasono et al., 2000). Then the linear system of equations (17) can be assembled and solved numerically for the coefficients of the polynomial expansion of the eigenstrain,  $\boldsymbol{\eta}_\alpha^{k_\bullet}$  [see Eq. (12)].

The EIM-T presented above has two shortcomings. First, there is no guarantee that the linear system given by Eq. (17) is indeed invertible; the EIM-T therefore lacks robustness, as it might fail in some circumstances. Second, increasing the degree  $p$  of the expansions does not necessarily improve the quality of the approximate solution given by Eqs. (12) and (13). This has already been reported by many authors (Rodin and Hwang, 1991;

Fond et al., 2001; Benedikt et al., 2006). Also, convergence (as  $p \rightarrow +\infty$ ) of this numerical method is not established.

In Sec. 3, an alternative to Taylor expansions is proposed to carry out the discretization of the consistency equation, and overcome these problems. Following a Galerkin approach based on the weak form of Eq. (11), a new system of equations is derived for the polynomial expansion of the unknown local polarization  $\boldsymbol{\tau}$ . This new system replaces the system obtained by Moschovidis and Mura [see Eq. (17)]; for this new system, well-posedness and convergence (as  $p \rightarrow +\infty$ ) to the true polarization can then be investigated with the help of standard mathematical tools [see e.g. Ern and Guermond (2004)].

Before this variational approach is introduced in Sec. 3, application of the EIM to homogenization problems is first discussed in Sec. 2.3. It is shown that a slight modification [introduced by Brisard et al. (2013b)] of the standard Lippmann–Schwinger equation (11) makes it much better-suited to this kind of problems. Galerkin discretization will therefore be carried out on the modified Lippmann–Schwinger equation [see Eq. (21)].

### 2.3. The EIM for numerical homogenization

Provided that the degree  $p$  of the polynomial expansions is not too high, each inhomogeneity has relatively few degrees of freedom; in other words, the linear system (17) remains small, even for large assemblies of inhomogeneities. The EIM is therefore an attractive tool for numerical homogenization, where hundreds to thousands of inhomogeneities must be considered simultaneously. Attention must however be paid to the boundary conditions, as was already noted by Fond et al. (2002).

We seek to determine (numerical estimates of) the apparent stiffness of a statistical volume element  $\Omega \subset \mathbb{R}^d$  [SVE, following the terminology of Ostoja-Starzewski (2006)]. As previously, the microstructure is formed of inhomogeneities  $\Omega_1, \dots, \Omega_N$  embedded in a homogeneous matrix. However, contrary to Sec. 2.2, the SVE  $\Omega$  is now a *bounded* domain.

It is recalled that the apparent stiffness  $\mathbf{C}^{\text{app}}$  relates the macroscopic stress  $\overline{\boldsymbol{\sigma}}$  to the macroscopic strain  $\overline{\boldsymbol{\varepsilon}}$

$$\overline{\boldsymbol{\sigma}} = \mathbf{C}^{\text{app}} : \overline{\boldsymbol{\varepsilon}}, \quad (18)$$

where overlined quantities denote volume averages over the bounded domain  $\Omega$

$$\overline{\boldsymbol{\varepsilon}} = \frac{1}{|\Omega|} \int_{\Omega} \boldsymbol{\varepsilon} \quad \text{and} \quad \overline{\boldsymbol{\sigma}} = \frac{1}{|\Omega|} \int_{\Omega} \boldsymbol{\sigma}.$$

In Eq. (18), the macroscopic strain and stress are computed from the solution to the following auxiliary problem, which states that the SVE is in (elastic) equilibrium (Fig. 2, left)

$$\begin{aligned} \nabla_{\mathbf{x}} \cdot \boldsymbol{\sigma} &= \mathbf{0} & (\mathbf{x} \in \Omega), \\ \boldsymbol{\sigma}(\mathbf{x}) &= \mathbf{C}(\mathbf{x}) : \boldsymbol{\varepsilon}(\mathbf{x}) & (\mathbf{x} \in \Omega), \\ \boldsymbol{\varepsilon}(\mathbf{x}) &= \nabla_{\mathbf{x}}^s \mathbf{u} & (\mathbf{x} \in \Omega). \end{aligned}$$

In addition, appropriate boundary conditions must be specified. The boundary conditions most frequently met are kinematic uniform (KUBC), static uniform (SUBC) and periodic (PBC)

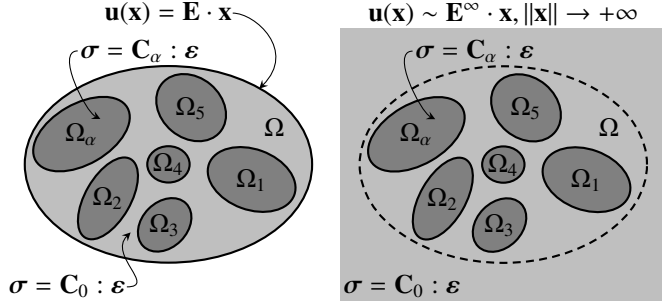


Figure 2: Left: evaluation of the apparent stiffness traditionally requires the determination of the elastic equilibrium of the SVE  $\Omega$ , with appropriate boundary conditions imposed at the boundary  $\partial\Omega$  (boundary conditions of type KUBC are represented here). Right: in order to evaluate the apparent stiffness by means of the EIM, the SVE  $\Omega$  must be embedded in an infinite homogeneous medium with same stiffness as the matrix, with imposed strain  $\mathbf{E}^\infty$  at infinity (boundary conditions of type KUBC $^\infty$ ). In this case, the loading parameter  $\mathbf{E}^\infty$  is *not* the macroscopic strain  $\bar{\boldsymbol{\varepsilon}}$ .

boundary conditions [see among others Hill (1963a, 1967), Mandel (1972) and Gusev (1997)]. With kinematic uniform and periodic boundary conditions, the loading parameter is the macroscopic strain ( $\mathbf{E} = \bar{\boldsymbol{\varepsilon}}$  is specified), while with static uniform boundary conditions, the loading parameter is the macroscopic stress ( $\boldsymbol{\Sigma} = \bar{\boldsymbol{\sigma}}$  is specified). For a finite-size SVE, these boundary conditions produce three different estimates of the apparent stiffness:  $\mathbf{C}_{\text{KUBC}}^{\text{app}}$ ,  $\mathbf{C}_{\text{SUBC}}^{\text{app}}$ ,  $\mathbf{C}_{\text{PBC}}^{\text{app}}$ . However, under statistical homogeneity and ergodicity assumptions, all estimates converge to the effective stiffness  $\mathbf{C}^{\text{eff}}$  as the size of the SVE tends to infinity (Sab, 1992).

As previously mentioned, the EIM is an attractive technique to compute numerical estimates of the apparent stiffness of the SVE  $\Omega$ . This would of course require to embed the bounded domain  $\Omega$  in an infinite, homogeneous medium with same stiffness as the matrix (Fig. 2, right). However, the EIM-T is a discretization of the  $N$ -inhomogeneity problem (3) with boundary conditions of type KUBC $^\infty$ , which is not strictly speaking a standard auxiliary problem, for two reasons. First, elastic equilibrium is specified in the whole space  $\mathbb{R}^d$  (as opposed to the bounded domain  $\Omega \subset \mathbb{R}^d$ ); second, neither macroscopic strain nor macroscopic stress can be specified. Indeed, there is no simple relationship between the sole loading parameter  $\mathbf{E}^\infty$  [see Eq. (3d)] and the macroscopic strain or stress (in particular,  $\bar{\boldsymbol{\varepsilon}} \neq \mathbf{E}^\infty$ ).

Notwithstanding, the  $N$ -inhomogeneity problem (3) can still be used to define an apparent stiffness  $\mathbf{C}_{\text{KUBC}^\infty}^{\text{app}}$  of the SVE  $\Omega$ . Indeed, from the linearity of this problem with respect to  $\mathbf{E}^\infty$ , both  $\bar{\boldsymbol{\sigma}}$  and  $\bar{\boldsymbol{\varepsilon}}$  depend linearly on the strain at infinity  $\mathbf{E}^\infty$

$$\bar{\boldsymbol{\varepsilon}} = \mathbf{A}_{\text{KUBC}^\infty} : \mathbf{E}^\infty, \quad \bar{\boldsymbol{\sigma}} = \mathbf{B}_{\text{KUBC}^\infty} : \mathbf{E}^\infty,$$

where  $\mathbf{A}_{\text{KUBC}^\infty}$  and  $\mathbf{B}_{\text{KUBC}^\infty}$  are fourth-rank localization tensors. The apparent stiffness results from the elimination of the loading parameter  $\mathbf{E}^\infty$  [see e.g. Fond et al. (2001, 2002)]

$$\mathbf{C}_{\text{KUBC}^\infty}^{\text{app}} = \mathbf{B}_{\text{KUBC}^\infty} : \mathbf{A}_{\text{KUBC}^\infty}^{-1}, \quad (19)$$

and this definition is consistent in the sense that  $\mathbf{C}_{\text{KUBC}^\infty}^{\text{app}} \rightarrow \mathbf{C}^{\text{eff}}$  as  $|\Omega| \rightarrow +\infty$  (under statistical homogeneity and ergodicity

assumptions). To sum up, the macroscopic strain and stress must be computed for six independent values of the loading parameter  $\mathbf{E}^\infty$  (strain at infinity); from these six computations, the localization tensors  $\mathbf{A}_{\text{KUBC}^\infty}$  and  $\mathbf{B}_{\text{KUBC}^\infty}$  can be computed, and the apparent stiffness  $\mathbf{C}_{\text{KUBC}^\infty}^{\text{app}}$  can be retrieved. However, evaluating  $\bar{\boldsymbol{\varepsilon}}$  and  $\bar{\boldsymbol{\sigma}}$  from the EIM estimate of the prestress involves complex surface integrals at the boundary  $\partial\Omega$  of the SVE (Fond et al., 2001, 2002). These operations are costly and potentially inaccurate. Furthermore, there is no guarantee that the apparent stiffness thus defined is symmetric, positive definite for finite-size SVEs. Using an energy approach to define the apparent stiffness partially resolves these issues (Rodin and Hwang, 1991).

Mixed boundary conditions (MBC) were introduced and analyzed in detail by Brisard et al. (2013b) as a way to circumvent the above-mentioned shortcomings of the boundary conditions of type KUBC $^\infty$ . The resulting system (20) of partial differential equations is very similar to the initial problem (3) with boundary conditions of type KUBC $^\infty$ . Yet, it is better-suited to homogenization problems, since the loading parameter  $\mathbf{E}$  is now the macroscopic strain [in other words, the solution to problem (20) satisfies  $\bar{\boldsymbol{\varepsilon}} = \mathbf{E}$ ]. Besides, the macroscopic stress can readily be derived from the average polarization, the computation of which does not involve complex surface integrals. Furthermore, the corresponding apparent stiffness is symmetric, positive definite, and we have

$$\mathbf{C}_{\text{SUBC}}^{\text{app}} \leq \mathbf{C}_{\text{MBC}}^{\text{app}} \leq \mathbf{C}_{\text{KUBC}}^{\text{app}},$$

where inequalities should be understood in the sense of quadratic forms.

The  $N$ -inhomogeneity problem with mixed boundary conditions is depicted in Fig. 3. The SVE  $\Omega$  is embedded in an infinite, homogeneous medium with same stiffness as the matrix. It is then submitted to a uniform strain  $\mathbf{E}$  at infinity, as well as a surface load  $\mathbf{t} \cdot \mathbf{n}$  applied to the boundary  $\partial\Omega$  of the SVE, where  $\mathbf{t}$  is a constant, second-rank, symmetric tensor and  $\mathbf{n}$  is the outward normal to  $\partial\Omega$

$$\nabla_{\mathbf{x}} \cdot \boldsymbol{\sigma} = \mathbf{0} \quad (\mathbf{x} \in \mathbb{R}^d), \quad (20a)$$

$$\boldsymbol{\sigma}(\mathbf{x}) = \mathbf{C}(\mathbf{x}) : \boldsymbol{\varepsilon}(\mathbf{x}) \quad (\mathbf{x} \in \mathbb{R}^d), \quad (20b)$$

$$\boldsymbol{\varepsilon}(\mathbf{x}) = \nabla_{\mathbf{x}}^s \mathbf{u} \quad (\mathbf{x} \in \mathbb{R}^d), \quad (20c)$$

$$\llbracket \boldsymbol{\sigma} \rrbracket(\mathbf{x}) \cdot \mathbf{n}(\mathbf{x}) = -\mathbf{t} \cdot \mathbf{n}(\mathbf{x}) \quad (\mathbf{x} \in \partial\Omega), \quad (20d)$$

$$\mathbf{u}(\mathbf{x}) \sim \mathbf{E} \cdot \mathbf{x} \quad (|\mathbf{x}| \rightarrow +\infty), \quad (20e)$$

$$\bar{\boldsymbol{\varepsilon}} = \mathbf{E}, \quad (20f)$$

where  $\llbracket \boldsymbol{\sigma} \rrbracket$  denotes the stress-jump across the boundary  $\partial\Omega$  of the SVE  $\Omega$ . From the above set of equations, it is apparent that  $\mathbf{t}$  is *not* a loading parameter, but should be chosen so as to ensure that Eq. (20f) holds. In other words, the unique loading parameter in the  $N$ -inhomogeneity problem with boundary conditions of type MBC is the strain at infinity  $\mathbf{E}$ , which is forced to coincide with the average strain over the SVE.

At first sight, problem (20) might seem more complex than problem (3) because of the additional unknown  $\mathbf{t}$ . However, it can be shown (Brisard et al., 2013b) that for ellipsoidal SVEs  $\Omega$ ,

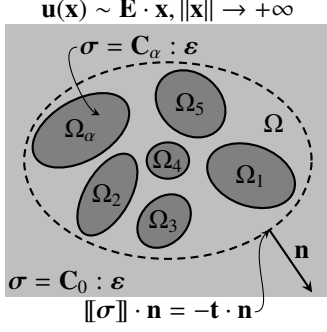


Figure 3: The  $N$ -inhomogeneity problem with mixed boundary conditions (MBC). Similarly to the situation depicted in Fig. 2 (right), the SVE  $\Omega$  is embedded in an infinite medium with same stiffness as the matrix. It is submitted to a uniform strain at infinity  $\mathbf{E}$ , as well as a surface load  $\mathbf{t} \cdot \mathbf{n}$  applied at the boundary  $\partial\Omega$  of the SVE  $\Omega$ . The constant, second-rank, symmetric tensor  $\mathbf{t}$  is a free parameter which is chosen so as to ensure that the unique loading parameter  $\mathbf{E}$  coincides with the macroscopic strain  $\bar{\boldsymbol{\varepsilon}}$ .

Eqs. (20) are equivalent to the following modified Lippmann–Schwinger equation, from which the supplementary unknown, constant tensor  $\mathbf{t}$  is absent

$$(\mathbf{C} - \mathbf{C}_0)^{-1} : \boldsymbol{\tau} + \boldsymbol{\Gamma}_0^\infty * (\boldsymbol{\tau} - \chi \bar{\boldsymbol{\tau}}) = \mathbf{E}, \quad (21)$$

where  $\chi$  denotes the indicator function of  $\Omega$  and  $\boldsymbol{\tau}$  again denotes the polarization [see Eq. (10)]. Furthermore, the local strain  $\boldsymbol{\varepsilon}$  and stress  $\boldsymbol{\sigma}$  are readily retrieved from the solution  $\boldsymbol{\tau}$  to Eq. (21) (Brisard et al., 2013b)

$$\boldsymbol{\varepsilon} = \mathbf{E} - \boldsymbol{\Gamma}_0^\infty * (\boldsymbol{\tau} - \chi \bar{\boldsymbol{\tau}}) \quad \text{and} \quad \boldsymbol{\sigma} = \mathbf{C}_0 : \boldsymbol{\varepsilon} + \boldsymbol{\tau}. \quad (22)$$

The above formulation as an integral equation shows that the  $N$ -inhomogeneity problems with boundary conditions of type MBC [see Eqs. (21) and (22)] and KUBC<sup>∞</sup> [see Eqs. (11) and (7)] are very similar, and can be discretized through the same techniques [including Taylor expansions used by Moschovidis and Mura (1975) for Eq. (9)]. From Eq. (22)<sub>2</sub> and the constraint  $\bar{\boldsymbol{\varepsilon}} = \mathbf{E}$ , the following identity is readily found

$$\bar{\boldsymbol{\tau}} = (\mathbf{C}_{\text{MBC}}^{\text{app}} - \mathbf{C}_0) : \mathbf{E}, \quad (23)$$

where  $\mathbf{C}_{\text{MBC}}^{\text{app}}$  denotes the apparent stiffness associated with mixed boundary conditions. As a consequence, unlike the original Lippmann–Schwinger equation (11), estimation of the apparent stiffness from a numerical solution to the modified Lippmann–Schwinger equation (21) does not involve complex surface integrals. Indeed, only the volume average of the polarization is required, which is trivial to compute provided a simple form is assumed for the numerical estimate of the polarization [see Eq. (26)]. Slightly modifying the equation to be solved numerically therefore allows to overcome one of the shortcomings of the EIM-T.

Adopting a Galerkin approach (rather than Taylor expansions) for the discretization of this equation allows to overcome all other shortcomings of the EIM-T listed in Sec. 2. This will be shown in Sec. 3, where a variational form of the EIM is proposed, based on the modified Lippmann–Schwinger equation (21), and piecewise polynomial approximations of the local polarization [see Eq. (26)].

To close this section, it should be noted that other types of mixed boundary conditions have been proposed in the past by various authors [see among others Hazanov and Huet (1994); Coenen et al. (2012); Salmi et al. (2012)]. However, such boundary conditions usually apply at the boundary  $\partial\Omega$  of the (bounded) SVE. This precludes the use of the Green operator for strains  $\boldsymbol{\Gamma}_0^\infty$  of the whole space to solve the underlying system of partial differential equations. By contrast, the mixed boundary conditions introduced in Brisard et al. (2013b) and used in the present paper apply partly at infinity. Eq. (21) shows that this approach allows to associate a very simple integral equation of the Lippmann–Schwinger type to the underlying (seemingly complex) system of partial differential equations (20). It should be emphasized that with these boundary conditions, the Green operator for strains  $\boldsymbol{\Gamma}_0^\infty$  of the whole space arises naturally, *without any approximation*. This is essential, since rigorous bounds on the apparent stiffness can then be produced through this approach, as shown in Sec. 3.2. Finally, the fact that the Green operator of the whole space (rather than the bounded SVE  $\Omega$ ) appears in the integral equation (21) is what makes the EIM practical. Indeed,  $\boldsymbol{\Gamma}_0^\infty$  has very simple expressions; besides, it is translation invariant, which makes assembly of the underlying linear system (37) [or indeed (17)] less costly.

### 3. Derivation of the proposed method

It is first noted that the equivalence between the  $N$ -inhomogeneity problem (20) with boundary conditions of type MBC and the modified Lippmann–Schwinger equation (21) holds for ellipsoidal SVEs only (Brisard et al., 2013b). Therefore, it will be assumed in the remainder of this paper that  $\Omega$  is an ellipsoid.

#### 3.1. Galerkin discretization of the consistency equation

The point of departure is the following weak form of the modified Lippmann–Schwinger equation (21), which is found by premultiplying with a test function  $\boldsymbol{\varpi} \in \mathbb{V}$ , and averaging over the SVE  $\Omega$

$$\text{Find } \boldsymbol{\tau} \in \mathbb{V} \text{ such that } a(\boldsymbol{\tau}, \boldsymbol{\varpi}) = f(\boldsymbol{\varpi}) \text{ for all } \boldsymbol{\varpi} \in \mathbb{V}, \quad (24)$$

where  $\mathbb{V}$  is the set of square integrable, second-rank, symmetric tensors, supported in  $\mathbb{R}^d \setminus \Omega_0$ ;  $a$  and  $f$  are bilinear and linear forms, respectively, given by

$$a(\boldsymbol{\tau}, \boldsymbol{\varpi}) = \overline{\boldsymbol{\varpi} : (\mathbf{C} - \mathbf{C}_0)^{-1} : \boldsymbol{\tau} + \boldsymbol{\varpi} : (\boldsymbol{\Gamma}_0^\infty * (\boldsymbol{\tau} - \chi \bar{\boldsymbol{\tau}}))}, \\ f(\boldsymbol{\varpi}) = \mathbf{E} : \bar{\boldsymbol{\varpi}}.$$

It should be noted that since the SVE  $\Omega$  is an ellipsoid, the theorem of Eshelby (1957) applies, and for all  $\mathbf{x} \in \Omega$

$$(\boldsymbol{\Gamma}_0^\infty * (\chi \bar{\boldsymbol{\tau}}))(\mathbf{x}) = \mathbf{P}_\Omega : \bar{\boldsymbol{\tau}},$$

where  $\mathbf{P}_\Omega$  denotes the Hill tensor of the domain  $\Omega$  with respect to the reference medium  $\mathbf{C}_0$ . Therefore, the bilinear form  $a$  reduces to

$$a(\boldsymbol{\tau}, \boldsymbol{\varpi}) = \overline{\boldsymbol{\varpi} : (\mathbf{C} - \mathbf{C}_0)^{-1} : \boldsymbol{\tau} + \boldsymbol{\varpi} : (\boldsymbol{\Gamma}_0^\infty * \boldsymbol{\tau})} - \bar{\boldsymbol{\varpi}} : \mathbf{P}_\Omega : \bar{\boldsymbol{\tau}}.$$



The above continuous variational problem is then discretized following a standard Galerkin procedure. More precisely, Eq. (24) is replaced with

$$\text{Find } \boldsymbol{\tau}^p \in \mathbb{V}^p \text{ such that } a(\boldsymbol{\tau}^p, \boldsymbol{\varpi}^p) = f(\boldsymbol{\varpi}^p) \text{ for all } \boldsymbol{\varpi}^p \in \mathbb{V}^p, \quad (25)$$

where  $\mathbb{V}^p$  is the finite dimension set of piecewise polynomial polarizations  $\boldsymbol{\tau}^p$  defined as follows

$$\boldsymbol{\tau}^p(\mathbf{x}) = \sum_{\alpha=1}^N \sum_{k_\bullet \in \mathfrak{S}^p} \chi_\alpha(\mathbf{x} - \mathbf{x}_\alpha) (x_\bullet - x_{\alpha,\bullet})^{k_\bullet} \boldsymbol{\tau}_\alpha^{k_\bullet}. \quad (26)$$

Comparison with Eqs. (10) and (12) shows that the present variational form of the EIM uses the same piecewise polynomial approximation of the polarization as the classical EIM of Moschovidis and Mura (1975).

The discrete variational problem (25) reduces to a linear system, with the coefficients  $\boldsymbol{\tau}_\alpha^{k_\bullet}$  of the polynomial expansion (26) as unknowns. Introducing the following expansion of the test function  $\boldsymbol{\varpi}^p \in \mathbb{V}^p$

$$\boldsymbol{\varpi}^p(\mathbf{x}) = \sum_{\alpha=1}^N \sum_{k_\bullet \in \mathfrak{S}^p} \chi_\alpha(\mathbf{x} - \mathbf{x}_\alpha) (x_\bullet - x_{\alpha,\bullet})^{k_\bullet} \boldsymbol{\varpi}_\alpha^{k_\bullet}, \quad (27)$$

the linear system to be solved is derived from the substitution of Eqs. (26) and (27) into Eq. (25). Recalling that all inclusions are completely included in  $\Omega$ , so that  $\int_\Omega \chi_\alpha = \int_{\mathbb{R}^d} \chi_\alpha$  ( $\alpha = 1, \dots, N$ ), it is readily found that

$$\overline{\boldsymbol{\varpi}^p} = \frac{1}{|\Omega|} \sum_{\alpha=1}^N \sum_{k_\bullet \in \mathfrak{S}^p} \mathcal{M}_\alpha^{k_\bullet} \boldsymbol{\varpi}_\alpha^{k_\bullet}, \quad (28)$$

where  $\mathcal{M}_\alpha^{k_\bullet}$  denotes the moment of order  $k_\bullet$  of inclusion  $\alpha$

$$\mathcal{M}_\alpha^{k_\bullet} = \int_{\mathbf{x} \in \mathbb{R}^d} \chi_\alpha(\mathbf{x}) x_\bullet^{k_\bullet} dV_{\mathbf{x}}. \quad (29)$$

Consequently, the value of the linear form  $f$  at  $\boldsymbol{\varpi}^p \in \mathbb{V}^p$  reads

$$f(\boldsymbol{\varpi}^p) = \frac{1}{|\Omega|} \sum_{\alpha=1}^N \sum_{k_\bullet \in \mathfrak{S}^p} \mathcal{M}_\alpha^{k_\bullet} \boldsymbol{\varpi}_\alpha^{k_\bullet} : \mathbf{E}. \quad (30)$$

Similarly

$$\begin{aligned} \overline{\boldsymbol{\varpi}^p} : (\mathbf{C} - \mathbf{C}_0)^{-1} : \boldsymbol{\tau}^p \\ = \frac{1}{|\Omega|} \sum_{\alpha=1}^N \sum_{k_\bullet, l_\bullet \in \mathfrak{S}^p} \mathcal{M}_\alpha^{k_\bullet+l_\bullet} \boldsymbol{\varpi}_\alpha^{k_\bullet} : (\mathbf{C}_\alpha - \mathbf{C}_0)^{-1} : \boldsymbol{\tau}_\alpha^{l_\bullet}, \end{aligned} \quad (31)$$

and

$$\overline{\boldsymbol{\varpi}^p} : (\boldsymbol{\Gamma}_0^\infty * \boldsymbol{\tau}^p) = \frac{1}{|\Omega|} \sum_{\alpha,\beta=1}^N \sum_{k_\bullet, l_\bullet \in \mathfrak{S}^p} \boldsymbol{\varpi}_\alpha^{k_\bullet} : \mathbf{T}_{\alpha\beta}^{k_\bullet, l_\bullet}(\mathbf{r}_{\alpha\beta}) : \boldsymbol{\tau}_\beta^{l_\bullet}, \quad (32)$$

where  $\mathbf{r}_{\alpha\beta} = \mathbf{x}_\beta - \mathbf{x}_\alpha$  and  $\mathbf{T}_{\alpha\beta}^{k_\bullet, l_\bullet}(\mathbf{r})$  denotes the following influence pseudotensor

$$\mathbf{T}_{\alpha\beta}^{k_\bullet, l_\bullet}(\mathbf{r}) = \int_{\mathbf{x}, \mathbf{y} \in \mathbb{R}^d} \chi_\alpha(\mathbf{x}) \chi_\beta(\mathbf{y}) x_\bullet^{k_\bullet} y_\bullet^{l_\bullet} \boldsymbol{\Gamma}_0^\infty(\mathbf{r} + \mathbf{y} - \mathbf{x}) dV_{\mathbf{x}} dV_{\mathbf{y}}. \quad (33)$$

For  $k_\bullet = l_\bullet = \mathbf{0}_\bullet$ , these pseudotensors coincide with  $\mathbf{T}^{II}$  and  $\mathbf{T}^{IJ}$  introduced by Berveiller et al. (1987) and Molinari and El Mouden (1996). It is assumed that the inclusions do not overlap. Therefore, if  $\alpha \neq \beta$ , then  $\mathbf{r} + \mathbf{y} - \mathbf{x}$  is always non-zero in the above integral, and the integrand is never singular. By contrast, if  $\alpha = \beta$ , then  $\mathbf{r} = \mathbf{0}$ , and the integrand is singular. This suggests to single out so-called self-influence pseudotensors, defined as follows

$$\mathbf{S}_\alpha^{k_\bullet, l_\bullet} = \mathbf{T}_{\alpha\alpha}^{k_\bullet, l_\bullet}(\mathbf{0}), \quad (34)$$

and it is noted that  $|\Omega_\alpha|^{-1} \mathbf{S}_\alpha^{0_\bullet, 0_\bullet}$  is the Hill tensor of inclusion  $\alpha$  with respect to the reference medium  $\mathbf{C}_0$ . Eq. (32) then reads

$$\begin{aligned} \overline{\boldsymbol{\varpi}^p} : (\boldsymbol{\Gamma}_0^\infty * \boldsymbol{\tau}^p) &= \frac{1}{|\Omega|} \sum_{\substack{\alpha,\beta=1 \\ \alpha \neq \beta}}^N \sum_{k_\bullet, l_\bullet \in \mathfrak{S}^p} \boldsymbol{\varpi}_\alpha^{k_\bullet} : \mathbf{T}_{\alpha\beta}^{k_\bullet, l_\bullet}(\mathbf{r}_{\alpha\beta}) : \boldsymbol{\tau}_\beta^{l_\bullet} \\ &+ \frac{1}{|\Omega|} \sum_{\alpha=1}^N \sum_{k_\bullet, l_\bullet \in \mathfrak{S}^p} \boldsymbol{\varpi}_\alpha^{k_\bullet} : \mathbf{S}_\alpha^{k_\bullet, l_\bullet} : \boldsymbol{\tau}_\alpha^{l_\bullet}, \end{aligned} \quad (35)$$

Evaluation of the bilinear form  $a$  for  $\boldsymbol{\tau}^p, \boldsymbol{\varpi}^p \in \mathbb{V}^p$  is then carried out from Eqs. (28), (31) and (35)

$$\begin{aligned} a(\boldsymbol{\tau}^p, \boldsymbol{\varpi}^p) &= \frac{1}{|\Omega|} \sum_{\alpha=1}^N \sum_{k_\bullet, l_\bullet \in \mathfrak{S}^p} \mathcal{M}_\alpha^{k_\bullet+l_\bullet} \boldsymbol{\varpi}_\alpha^{k_\bullet} : (\mathbf{C}_\alpha - \mathbf{C}_0)^{-1} : \boldsymbol{\tau}_\alpha^{l_\bullet} \\ &+ \frac{1}{|\Omega|} \sum_{\alpha=1}^N \sum_{k_\bullet, l_\bullet \in \mathfrak{S}^p} \boldsymbol{\varpi}_\alpha^{k_\bullet} : \mathbf{S}_\alpha^{k_\bullet, l_\bullet} : \boldsymbol{\tau}_\alpha^{l_\bullet} \\ &+ \frac{1}{|\Omega|} \sum_{\substack{\alpha,\beta=1 \\ \alpha \neq \beta}}^N \sum_{k_\bullet, l_\bullet \in \mathfrak{S}^p} \boldsymbol{\varpi}_\alpha^{k_\bullet} : \mathbf{T}_{\alpha\beta}^{k_\bullet, l_\bullet}(\mathbf{r}_{\alpha\beta}) : \boldsymbol{\tau}_\beta^{l_\bullet} \\ &- \frac{1}{|\Omega|^2} \sum_{\alpha,\beta=1}^N \sum_{k_\bullet, l_\bullet \in \mathfrak{S}^p} \mathcal{M}_\alpha^{k_\bullet} \mathcal{M}_\beta^{l_\bullet} \boldsymbol{\varpi}_\alpha^{k_\bullet} : \mathbf{P}_\Omega : \boldsymbol{\tau}_\beta^{l_\bullet}. \end{aligned} \quad (36)$$

Gathering Eqs. (30) and (36), it is found that the discretized variational problem (25) is equivalent to the following linear system with unknowns  $\boldsymbol{\tau}_\alpha^{k_\bullet}$  (one equation for each value of  $\alpha = 1, \dots, N$  and  $k_\bullet \in \mathfrak{S}^p$ )

$$\begin{aligned} \sum_{l_\bullet \in \mathfrak{S}^p} \left( \mathcal{M}_\alpha^{k_\bullet+l_\bullet} (\mathbf{C}_\alpha - \mathbf{C}_0)^{-1} + \mathbf{S}_\alpha^{k_\bullet, l_\bullet} - \frac{\mathcal{M}_\alpha^{k_\bullet} \mathcal{M}_\alpha^{l_\bullet}}{|\Omega|} \mathbf{P}_\Omega \right) : \boldsymbol{\tau}_\alpha^{l_\bullet} \\ + \sum_{\substack{\beta=1 \\ \beta \neq \alpha}}^N \sum_{l_\bullet \in \mathfrak{S}^p} \left( \mathbf{T}_{\alpha\beta}^{k_\bullet, l_\bullet}(\mathbf{r}_{\alpha\beta}) - \frac{\mathcal{M}_\alpha^{k_\bullet} \mathcal{M}_\beta^{l_\bullet}}{|\Omega|} \mathbf{P}_\Omega \right) : \boldsymbol{\tau}_\beta^{l_\bullet} = \mathcal{M}_\alpha^{k_\bullet} \mathbf{E}. \end{aligned} \quad (37)$$

For inhomogeneities with simple geometries, closed-form expressions of the moments  $\mathcal{M}_\alpha^{k_\bullet}$ , self-influence pseudotensors  $\mathbf{S}_\alpha^{k_\bullet, l_\bullet}$  and influence pseudotensors  $\mathbf{T}_{\alpha\beta}^{k_\bullet, l_\bullet}(\mathbf{r})$  can be derived (see Sec. 4); assembly of the above system is therefore straightforward. Following an approach similar to that of Brisard and Dormieux (2012) (see in particular Sec. 4.2 in this reference), it can be shown that this system is well-posed.

To sum up, the EIM-G is defined through the discretization (26) and the linear system (37). The solution to this system

provides the coefficients of the expansion of the approximate polarization,  $\boldsymbol{\tau}^p$ . In turn, estimates of the strain and stress in the inclusions can be computed as follows

$$\boldsymbol{\varepsilon}^p(\mathbf{x}) = (\mathbf{C}_\alpha - \mathbf{C}_0)^{-1} : \boldsymbol{\tau}^p(\mathbf{x}) \quad (\mathbf{x} \in \Omega_\alpha), \quad (38)$$

and

$$\boldsymbol{\sigma}^p(\mathbf{x}) = \mathbf{C}_0 : \boldsymbol{\varepsilon}^p(\mathbf{x}) + \boldsymbol{\tau}^p(\mathbf{x}) \quad (\mathbf{x} \in \Omega_\alpha).$$

For points belonging to the matrix, Eq. (38) is meaningless (since  $\mathbf{C} - \mathbf{C}_0$  is singular), and the approximate strains must be computed from the convolution product  $\boldsymbol{\varepsilon}^p = \mathbf{E} - \boldsymbol{\Gamma}_0^\infty * \boldsymbol{\tau}^p$ ; this involves complex numerical integration, which are not necessary for the determination of the approximate apparent stiffness,  $\mathbf{C}_{\text{MBC}}^{\text{app},p}$ . Indeed, from Eq. (23)

$$\mathbf{C}_{\text{MBC}}^{\text{app},p} : \mathbf{E} = \mathbf{C}_0 : \mathbf{E} + \overline{\boldsymbol{\tau}^p} = \mathbf{C}_0 : \mathbf{E} + \frac{1}{|\Omega|} \sum_{\alpha=1}^N \sum_{k_\alpha \in \mathfrak{S}^p} \mathcal{M}_\alpha^{k_\alpha} \boldsymbol{\tau}_\alpha^{k_\alpha}. \quad (39)$$

To close this section, it should be noted that for  $p = 0$  (constant polarization in each inclusion), the equations of the EIM-G are very close to those found by previous authors (Rodin and Hwang, 1991; Rodin, 1993; Molinari and El Mouden, 1996; El Mouden and Molinari, 2000). In the present work however, periodization of the unit-cell is not necessary owing to the introduction of the mixed boundary conditions and the corresponding correction term involving the Hill tensor  $\mathbf{P}_\Omega$  of the domain  $\Omega$  [see Eq. (36)].

### 3.2. Bounds on the apparent stiffness

Provided that the matrix is stiffer (resp. softer) than all inhomogeneities, the above approach leads to an upper bound (resp. lower bound) on the apparent stiffness of the SVE  $\Omega$ . Indeed, an extremum principle of the Hashin and Shtrikman (1962a) type has been proved for the modified Lippmann–Schwinger equation (21) (Brisard et al., 2013b). More precisely, introducing for  $\boldsymbol{\varpi} \in \mathbb{V}$  the following functional

$$\mathcal{H}(\boldsymbol{\varpi}) = f(\boldsymbol{\varpi}) - \frac{1}{2} a(\boldsymbol{\varpi}, \boldsymbol{\varpi}),$$

it can readily be shown that  $\mathcal{H}$  is stationary at the solution  $\boldsymbol{\tau}$  to Eq. (21), and

$$\mathcal{H}(\boldsymbol{\tau}) = \frac{1}{2} \mathbf{E} : (\mathbf{C}_{\text{MBC}}^{\text{app}} - \mathbf{C}_0) : \mathbf{E}. \quad (40)$$

It was further shown in (Brisard et al., 2013b) that  $\mathcal{H}$  is minimum (resp. maximum) at  $\boldsymbol{\tau}$ , provided  $\mathbf{C}_\alpha \leq \mathbf{C}_0$  (resp.  $\mathbf{C}_\alpha \geq \mathbf{C}_0$ ) for all  $\alpha = 1, \dots, N$ .

In particular, if one of these conditions is fulfilled,  $\mathcal{H}(\boldsymbol{\tau})$  can be compared to  $\mathcal{H}(\boldsymbol{\tau}^p)$ , where  $\boldsymbol{\tau}^p$  is the EIM-G estimate of  $\boldsymbol{\tau}$ . Since  $\boldsymbol{\tau}^p$  is the solution to the discretized variational problem (25), it verifies  $a(\boldsymbol{\tau}^p, \boldsymbol{\tau}^p) = f(\boldsymbol{\tau}^p)$ , and from Eq. (39), it is readily found that

$$\mathcal{H}(\boldsymbol{\tau}^p) = \frac{1}{2} \mathbf{E} : (\mathbf{C}_{\text{MBC}}^{\text{app},p} - \mathbf{C}_0) : \mathbf{E}. \quad (41)$$

If the matrix is stiffer than all inhomogeneities, then  $\mathcal{H}$  is minimum at  $\boldsymbol{\tau}$ , and  $\mathcal{H}(\boldsymbol{\tau}) \leq \mathcal{H}(\boldsymbol{\tau}^p)$ . Gathering Eqs. (40) and (41)

$$\mathbf{C}_{\text{MBC}}^{\text{app}} \leq \mathbf{C}_{\text{MBC}}^{\text{app},p},$$

the EIM-G estimate of the apparent stiffness is in fact an upper bound. Conversely, if the matrix is softer than all inhomogeneities, then the EIM-G estimate of the apparent stiffness is a lower bound.

To sum up, if the matrix is stiffer (resp. softer) than the inhomogeneities, then the variational form of the EIM returns upper (resp. lower) bounds on the apparent stiffness. This result further guarantees that the quality of the solution will not deteriorate as the order  $p$  of the method is increased. Indeed, the discretized variational problem (25) can be seen as the optimization of  $\mathcal{H}$  over the finite-dimension subspace  $\mathbb{V}^p$  of  $\mathbb{V}$ . As  $p$  grows, so does the subspace  $\mathbb{V}^p$ , and the quality of the approximate optimum is therefore improved. This desirable property is not necessarily observed with the EIM-T (Fond et al., 2001), which is not based on a variational setting.

## 4. Implementation of the method

The key point for the implementation of the method is the computation of the self-influence and influence pseudotensors. The complex integrals involved [see Eqs. (33) and (34)] must be evaluated with the help of a computer algebra system<sup>1</sup>. Examples of such computations can be found in Brisard et al. (2013a).

### 4.1. Computation of the self-influence pseudotensors

The self-influence pseudotensors  $\mathbf{S}_\alpha^{k_\alpha, l_\alpha}$  are defined as follows [see Eqs. (33) and (34)]

$$\mathbf{S}_\alpha^{k_\alpha, l_\alpha} = \int_{\mathbf{x}, \mathbf{y} \in \mathbb{R}^d} \chi_\alpha(\mathbf{x}) \chi_\alpha(\mathbf{y}) x_\alpha^{k_\alpha} y_\alpha^{l_\alpha} \boldsymbol{\Gamma}_0^\infty(\mathbf{y} - \mathbf{x}) dV_x dV_y.$$

In the above expression, principal values are taken according to Eq. (A.1) in order to remove the singularity at  $\mathbf{x} = \mathbf{y}$

$$\begin{aligned} \mathbf{S}_\alpha^{k_\alpha, l_\alpha} = & \int_{\mathbf{x} \in \mathbb{R}^d} \chi_\alpha(\mathbf{x}) x_\alpha^{k_\alpha} \lim_{\delta \rightarrow 0} \int_{\substack{\mathbf{y} \in \mathbb{R}^d \\ \|\mathbf{y} - \mathbf{x}\| > \delta}} \chi_\alpha(\mathbf{y}) y_\alpha^{l_\alpha} \mathbf{Q}_0(\mathbf{y} - \mathbf{x}) dV_y dV_x \\ & + \int_{\mathbf{x} \in \mathbb{R}^d} \chi_\alpha(\mathbf{x}) x_\alpha^{k_\alpha + l_\alpha} \mathbf{P}_0 dV_x. \end{aligned} \quad (42)$$

The last term reduces to  $\mathcal{M}_\alpha^{k_\alpha + l_\alpha} \mathbf{P}_0$ . For convex inclusions, the following change of variables is performed to compute the first term (see Fig. 4 and Appendix B.1 for more details)

$$\mathbf{y} = \mathbf{x} + r\mathbf{n}, \quad \text{with } \|\mathbf{n}\| = 1 \text{ and } 0 \leq r \leq R_\alpha(\mathbf{x}, \mathbf{n}), \quad (43)$$

<sup>1</sup>The present work was carried out with the Maxima computer algebra system, version 5.30.0, <http://maxima.sourceforge.net/> (last visited 2013-06-05).

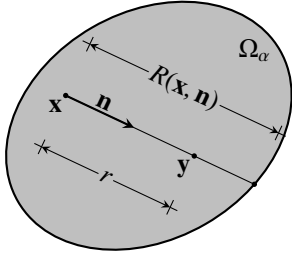


Figure 4: Variables for the calculation of the self-influence pseudotensor of inclusion  $\Omega_\alpha$ .

where  $R_\alpha(\mathbf{x}, \mathbf{n})$  is defined as the largest value of  $r$  such that  $\chi_\alpha(\mathbf{x} + r\mathbf{n}) = 1$  for  $\chi_\alpha(\mathbf{x}) = 1$ . It can then be shown that

$$\begin{aligned} \mathbf{S}_\alpha^{k_\bullet, l_\bullet} &= \mathcal{M}_\alpha^{k_\bullet + l_\bullet} \mathbf{P}_0 \\ &+ \int_{\mathbf{x}, \mathbf{y} \in \mathbb{R}^d} \chi_\alpha(\mathbf{x}) \chi_\alpha(\mathbf{y}) x_\bullet^{k_\bullet} (y_\bullet^{l_\bullet} - x_\bullet^{l_\bullet}) \mathbf{Q}_0(\mathbf{y} - \mathbf{x}) dV_\mathbf{y} dV_\mathbf{x} \\ &+ \int_{\substack{\mathbf{x} \in \mathbb{R}^d \\ \|\mathbf{n}\|=1}} \chi_\alpha(\mathbf{x}) x_\bullet^{k_\bullet + l_\bullet} \log R_\alpha(\mathbf{x}, \mathbf{n}) \mathbf{Q}_0(\mathbf{n}) dS_\mathbf{n} dV_\mathbf{x}, \end{aligned} \quad (44)$$

where  $dS_\mathbf{n}$  denotes the surface element at  $\mathbf{n}$  on the unit sphere. For spherical inclusions, the last term vanishes, while the second term can be computed analytically (see [Appendix B.2](#)).

#### 4.2. Computation of the influence pseudotensors

The influence pseudotensors  $\mathbf{T}_{\alpha\beta}^{k_\bullet, l_\bullet}(\mathbf{r})$  are given by Eq. (33) (see also Fig. 5). As inclusions  $\alpha$  and  $\beta$  do not overlap, only the regular part  $\mathbf{Q}_0$  of  $\mathbf{\Gamma}_0^\infty$  is involved in this computation [see Eq. (A.1)].

Direct evaluation of integral (33) is complex (if possible at all). In particular, the method proposed by [Berveiller et al. \(1987\)](#)—based on Fourier transforms—for the evaluation of the lowest-order influence pseudotensor  $\mathbf{T}_{\alpha\beta}^{k_\bullet, l_\bullet}(\mathbf{r})$  with  $k_\bullet = l_\bullet = 0_\bullet$  does not generalize to higher orders. In the present paragraph, an alternative approach is therefore proposed, based on multipole expansions.

Let  $\mathbf{r} = r\mathbf{n}$  ( $\|\mathbf{n}\| = 1$ ) be a fixed vector, and  $\mathbf{r}' = r(\mathbf{n} + \boldsymbol{\xi})$ . From the homogeneity of degree  $-d$  of the regular part  $\mathbf{Q}_0$  of  $\mathbf{\Gamma}_0^\infty$ , it is found that

$$\mathbf{Q}_0(\mathbf{r}') = r^{-d} \mathbf{Q}_0(\mathbf{n} + \boldsymbol{\xi}),$$

which is expanded in a Taylor series with respect to the powers of the components of  $\boldsymbol{\xi}$ . The resulting expansion is then inserted in Eq. (33), with  $\boldsymbol{\xi} = (\mathbf{y} - \mathbf{x})/r$ . Each term of the series being a monomial in the variables  $x_i/r$  and  $y_j/r$  ( $i, j = 1, \dots, d$ ), its integral for  $\mathbf{x} \in \Omega_\alpha$  and  $\mathbf{y} \in \Omega_\beta$  can readily be computed (provided  $\Omega_\alpha$  and  $\Omega_\beta$  have simple shapes).

This procedure returns the influence pseudotensors  $\mathbf{T}_{\alpha\beta}^{k_\bullet, l_\bullet}(\mathbf{r})$  as series of the negative powers of  $r$ . In practice, this series must be truncated, and the above method ought to be viewed as approximate. However, experience shows that for spherical inclusions, all computed expansions have a finite number of non-zero terms. This suggests that the present computation would

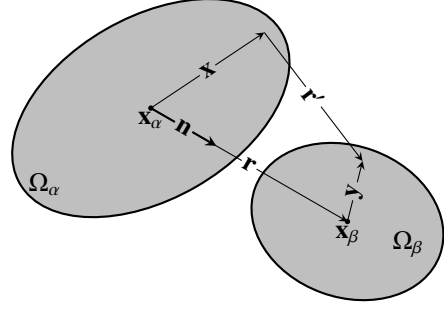


Figure 5: Variables for the calculation of the influence pseudotensor of inclusions  $\Omega_\alpha$  and  $\Omega_\beta$ .

in fact be exact in that case, although this conjecture remains unproved for the time being.

The above procedure involves rather tedious, but very systematic, algebra. As such, it lends itself to straightforward implementation in a computer algebra system; the resulting expressions are then imported into a numerical code, in charge of assembling and inverting the global matrix.

While it is possible to compute literal expressions of the influence tensors in any basis, the resulting expressions are intractable, and lead to cluttered code. For the sake of clarity and simplicity, closed-form expressions of the influence tensors were computed in a *local* basis ( $\mathbf{e}'_1, \dots, \mathbf{e}'_d$ ), where the  $d$ -th direction  $\mathbf{e}'_d$  coincides with the line of centers of the two inclusions ( $\mathbf{r} = r\mathbf{e}'_d$ ); the resulting pseudotensors are denoted  $\mathbf{T}_{\alpha\beta}^{k_\bullet, l_\bullet}(\mathbf{r})$ . A change of basis must be performed to retrieve the components of  $\mathbf{T}_{\alpha\beta}^{k_\bullet, l_\bullet}$  in the global basis ( $\mathbf{e}_1, \dots, \mathbf{e}_d$ ); this is performed numerically, during the assembly of the global matrix. It should be noted that this change of basis does not reduce to a standard linear algebra operation, since  $\mathbf{T}_{\alpha\beta}^{k_\bullet, l_\bullet}$  is not a tensor (see [Appendix C](#)).

## 5. Applications

In the present section, two applications of the variational form of the equivalent inclusion method (EIM-G) derived in Secs. 3 and 4 are proposed. The first application (see Sec. 5.1) is a plane strain elasticity application, while the second application (see Sec. 5.2) is a 3D elasticity application.

It is recalled that the EIM-G requires the SVE to be of ellipsoidal shape ([Brisard et al., 2013b](#)). Therefore, circular (resp. spherical) SVEs are considered in Sec. 5.1 (resp. 5.2).

### 5.1. Monodisperse assemblies of circular pores in plane strain elasticity

The present example deals with porous media in plane strain elasticity. The circular SVE  $\Omega$  contains  $N$  circular pores of radius  $a$ . The porosity is  $\phi = 0.4$ ; with  $N = 160$  pores, the radius  $R$  of the SVE  $\Omega$  is  $R = 20a$  (see Fig. 6). The shear modulus and Poisson ratio of the matrix are  $\mu_0$  (arbitrary value) and  $\nu_0 = 0.3$ .

To account for statistical fluctuations of the apparent mechanical properties of each individual SVE, 1 000 configurations were considered. The (mean) apparent shear modulus of these

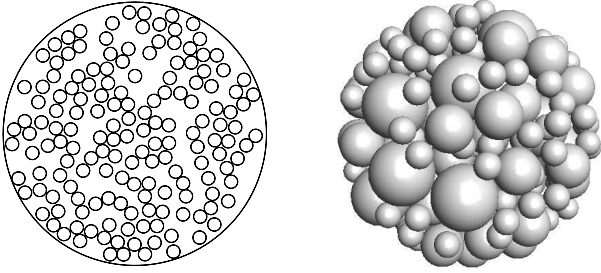


Figure 6: Left: graphical representation of one out of the 1 000 SVEs considered in Sec. 5.1. Circular, monodisperse pores are embedded in a homogeneous matrix; the porosity is  $\phi = 0.4$ . Right: graphical representation of one out of the 100 SVEs considered in Sec. 5.2. Spherical, polydisperse pores are embedded in a homogeneous matrix (only the pores are shown in this image); the porosity is  $\phi = 0.45$ .

Order $p$	Bound on $\mu^{\text{app}}$	DOFs
0	$0.310 \mu_0$	480
1	$0.278 \mu_0$	1 440
2	$0.257 \mu_0$	2 880
3	$0.247 \mu_0$	4 800

Table 1: Upper bounds on the apparent shear modulus of a monodisperse assembly of circular pores in plane strain elasticity, for increasing orders  $p$  of the EIM-G. For each value of  $p$ , the corresponding number of degrees of freedom (DOFs) is also reported.

microstructures is then estimated through the EIM-G, and the results are reported in Table 1 for various values of  $p$  (it is recalled that  $p$  is the maximum degree of the polynomial expansions used to approximate the polarization  $\tau$ ). Due to the large number of independent configurations considered here, the amplitude of the 99 % confidence interval is smaller than one unit in the last place of each value reported in Table 1.

Since the reference medium (the matrix) is stiffer than the inclusions, results presented in Sec. 3.2 apply, and the estimates of  $\mu^{\text{app}}$  are in fact upper bounds on this quantity. This is consistent with the fact that this bound decreases as  $p$  increases, as expected (the functional  $\mathcal{H}$  is minimized on sub-spaces of increasing dimension).

Observation of the results presented in Table 1 shows that increasing  $p$  significantly improves the upper bound on  $\mu^{\text{app}}$ . Indeed, from  $p = 0$  to  $p = 3$ , the upper-bound is reduced by approximately 20 %, while the total number of degrees of freedom is multiplied by a factor 10.

In order to quantify the error on the apparent shear modulus, the above results were compared to finite element (FEM) estimates computed on the same 1 000 configurations. Strictly speaking, EIM-G and FEM computations are not equivalent. Indeed, kinematic uniform boundary conditions were adopted for convenience for the FEM models, while EIM-G models require mixed boundary conditions (see Sec. 2.3 for a definition of these two types of boundary conditions). Since the SVEs under consideration are very large ( $R/a = 20$ ), finite-size effects should be negligible, and the apparent shear moduli resulting from these two sets of boundary conditions are expected to coincide (Hill, 1963a).

The FEM estimate of the apparent shear modulus was found

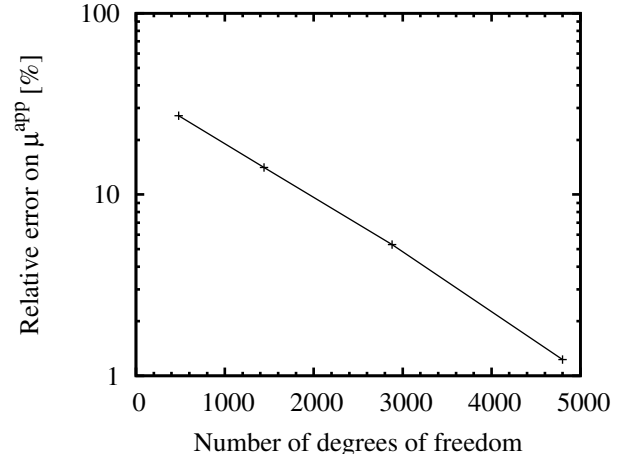


Figure 7: Relative error on  $\mu^{\text{app}}$  as a function of the number of degrees of freedom of the EIM-G, in semi-log scale. Convergence seems to be exponential.

to be  $0.244 \mu_0$ ; again, the 99 % confidence interval is narrow enough to ensure that this value is correct up to one unit in the last place. Using this value as a reference, Fig. 7 shows in semi-log scale the relative error on  $\mu^{\text{app}}$  as a function of the number of degrees of freedom. Observing Fig. 7, it seems that the EIM-G converges exponentially with respect to the number of degrees of freedom. This empirical result was expected, as similar asymptotic behaviors are also observed with the  $p$ -version of the FEM, which is very similar in spirit to EIM-G (Szabó et al., 2004).

Comparison of the respective sizes of the EIM-G and FEM models emphasizes the efficiency of the EIM-G. Indeed, each of the 1 000 FEM model contained about 320 000 degrees of freedom (this figure was variable from one configuration to another), while with only 4 800 degrees of freedom, the EIM-G achieves a relative error of approximately 1.2 %. In other words, the EIM-G can provide at a relatively low cost estimates of some quantities of interest with a small (but finite) error. Of course, if high accuracy is required, then the FEM should be preferred to the EIM-G.

To close this section, it should also be noted that the Hashin and Shtrikman (1962b) upper-bound on  $\mu^{\text{app}}$  reads in this case:  $\mu^{\text{HS}+} = 0.349 \mu_0$ . Clearly, this bound is a poor estimate in plane strain elasticity of the effective shear modulus of a composite with circular inclusions. Even the 0-th order EIM-G bound leads to an improvement of 11 %.

## 5.2. Polydisperse assembly of spherical pores in 3D elasticity

The present example deals with porous media in 3D elasticity. The spherical SVE  $\Omega$  contains  $N_1 = 20$  (resp.  $N_2 = 40$ ,  $N_3 = 140$ ) spherical pores of radius  $a_1$  (resp.  $a_2 = 0.7 a_1$ ,  $a_3 = 0.4 a_1$ ). The total porosity is  $\phi = 0.45$ , so that the radius  $R$  of the SVE  $\Omega$  is  $R = 4.56 a_1$  (see Fig. 6, right). The shear modulus and Poisson ratio of the matrix are  $\mu_0$  (arbitrary value) and  $\nu_0 = 0.3$ .

To account for statistical fluctuations, 100 such SVEs were generated. It should be noted that fluctuations were smaller in the present, 3D case than in the previous, plane strain one. In

Order $p$	Bound on $\mu^{\text{app}}$	DOFs
0	0.381	1 200
1	0.371	4 800
2	0.363	12 200

Table 2: Upper bounds on the apparent shear modulus of a polydisperse assembly of spherical pores in 3D elasticity, for increasing orders  $p$  of the EIM-G. For each value of  $p$ , the corresponding number of degrees of freedom (DOFs) is also reported.

both cases, the amplitude of the statistical error (99 % confidence interval) was identical, even if the number of generated configurations was ten times smaller in the 3D application.

The (mean) apparent shear modulus  $\mu^{\text{app}}$  of these microstructures is then estimated through the EIM-G, and the results are reported in Table 2 for various values of  $p$ . Again, the results are accurate (with probability 99 %) within one unit in the last place. For the same reasons as previously, they can be considered as upper bounds on  $\mu^{\text{app}}$  (which is again consistent with the fact that this bound decreases as  $p$  increases).

However, observing Table 2, it seems that the relative improvement of the bounds is much lower in the present case than in the previous, plane strain case, for the same increase of the number of degrees of freedom. It is necessary to thoroughly investigate this apparent loss of efficiency; this investigation will be carried out in future work.

## 6. Conclusion

In the present paper, we proposed a new form of the equivalent inclusion method (EIM). Recognizing that the EIM can be seen as an approximation of the Lippmann–Schwinger equation, we proposed a Galerkin discretization of the *weak* form of this integral equation as an alternative to the discretization of its *strong* form, based on Taylor expansions, initially proposed by Moschovidis and Mura (1975). All details are provided for the implementation of this new method.

Combined with the new, mixed boundary conditions recently introduced by the authors (Brisard et al., 2013b), the resulting numerical method is an attractive tool for homogenization. In particular, provided that the matrix is stiffer or softer than all inhomogeneities, it can provide rigorous bounds on the macroscopic properties, at a relatively low cost. Numerical examples show that the method is extremely efficient in plane strain elasticity, less so in three dimensional elasticity. We intend to investigate in future work the origins of this loss of efficiency, and how to overcome it. We will also extend the method to ellipsoidal inhomogeneities, which should allow us to capture local orientational order effects.

### Appendix A. On the infinite body Green’s operator for strains

It is recalled that the Green’s operator for strains  $\Gamma_0^\infty$  decomposes into a regular part  $\mathbf{Q}_0$  and a singular part  $\mathbf{P}_0$

$$(\Gamma_0^\infty * \boldsymbol{\tau})(\mathbf{x}) = \lim_{\delta \rightarrow 0} \int_{\substack{\mathbf{y} \in \Omega \\ \|\mathbf{y} - \mathbf{x}\| \geq \delta}} \mathbf{Q}_0(\mathbf{x} - \mathbf{y}) : \boldsymbol{\tau}(\mathbf{y}) dV_{\mathbf{y}} + \mathbf{P}_0 : \boldsymbol{\tau}(\mathbf{x}), \quad (\text{A.1})$$

where  $\mathbf{P}_0$  is the Hill tensor of  $d$ -dimensional spheres. Litteral expressions of  $\mathbf{P}_0$  and  $\mathbf{Q}_0(\mathbf{r})$  can be found in reference textbooks [see e.g. Torquato (2002); Buryachenko (2007); Kanaun and Levin (2008)]. For  $d = 3$ ,

$$\mathbf{P}_0 = \frac{1 - 2\nu_0}{6\mu_0(1 - \nu_0)} \mathbf{J} + \frac{4 - 5\nu_0}{15\mu_0(1 - \nu_0)} \mathbf{K}, \quad (\text{A.2})$$

and

$$\begin{aligned} \mathbf{Q}_0(\mathbf{r}) = & \frac{1}{16\pi\mu_0(1 - \nu_0)r^3} \left[ -\delta_{ij}\delta_{kl} + (1 - 2\nu_0)(\delta_{ik}\delta_{jl} + \delta_{il}\delta_{jk}) \right. \\ & + 3(\delta_{ij}n_k n_l + \delta_{kl}n_i n_j) \\ & + 3\nu_0(\delta_{ik}n_j n_l + \delta_{il}n_j n_k + \delta_{jk}n_i n_l + \delta_{jl}n_i n_k) \\ & \left. - 15n_i n_j n_k n_l \right] \mathbf{e}_i \otimes \mathbf{e}_j \otimes \mathbf{e}_k \otimes \mathbf{e}_l, \end{aligned} \quad (\text{A.3})$$

where  $\mu_0$  (resp.  $\nu_0$ ) is the shear modulus (resp. Poisson ratio) of the reference medium,  $r = \|\mathbf{r}\|$ ,  $\mathbf{n} = \mathbf{r}/r$  and  $\mathbf{J}$  (resp.  $\mathbf{K}$ ) is the spherical (resp. deviatoric) fourth-rank projection tensor. More precisely,  $\mathbf{J} = \frac{1}{d} \mathbf{i} \otimes \mathbf{i}$  and  $\mathbf{K} = \mathbf{I} - \mathbf{J}$ , where  $\mathbf{i}$  (resp.  $\mathbf{I}$ ) is the second- (resp. fourth-) rank identity tensor. For  $d = 2$  (plane strain elasticity),

$$\mathbf{P}_0 = \frac{1 - 2\nu_0}{4\mu_0(1 - \nu_0)} \mathbf{J} + \frac{3 - 4\nu_0}{8\mu_0(1 - \nu_0)} \mathbf{K}, \quad (\text{A.4})$$

and

$$\begin{aligned} \mathbf{Q}_0(\mathbf{r}) = & \frac{1}{8\pi\mu_0(1 - \nu_0)r^2} \left[ -\delta_{ij}\delta_{kl} + (1 - 2\nu_0)(\delta_{ik}\delta_{jl} + \delta_{il}\delta_{jk}) \right. \\ & + 2(\delta_{ij}n_k n_l + \delta_{kl}n_i n_j) \\ & + 2\nu_0(\delta_{ik}n_j n_l + \delta_{il}n_j n_k + \delta_{jk}n_i n_l + \delta_{jl}n_i n_k) \\ & \left. - 8n_i n_j n_k n_l \right] \mathbf{e}_i \otimes \mathbf{e}_j \otimes \mathbf{e}_k \otimes \mathbf{e}_l. \end{aligned} \quad (\text{A.5})$$

It should be observed that  $\mathbf{Q}_0$  is homogeneous of degree  $-d$ . Besides, the following identity will prove useful in the present paper

$$\int_{\|\mathbf{n}\|=1} \mathbf{Q}_0(\mathbf{n}) dS_{\mathbf{n}} = \mathbf{0}, \quad (\text{A.6})$$

where  $dS_{\mathbf{n}}$  denotes the surface element at  $\mathbf{n}$  on the unit sphere.

### Appendix B. Computation of the self-influence pseudotensors

In this section, a procedure is presented for the computation of the self-influence pseudotensors of spherical inclusions. The general expression [see Eq. (42)] of the self-influence pseudotensors is first transformed so as to handle the principal values (see Appendix B.1). It is then shown that the resulting integral can be computed analytically in the case of spherical inclusions (see Appendix B.2).

### Appendix B.1. Proof of Eq. (44)

These pseudotensors are defined by Eq. (42), where the principal value must be computed. Let

$$\mathbf{Q}_\alpha^{l_\bullet}(\mathbf{x}) = \lim_{\delta \rightarrow 0} \int_{\substack{\mathbf{y} \in \mathbb{R}^d \\ \|\mathbf{y} - \mathbf{x}\| > \delta}} \chi_\alpha(\mathbf{y}) \mathbf{y}^{l_\bullet} \mathbf{Q}_0(\mathbf{y} - \mathbf{x}) dV_{\mathbf{y}}, \quad (\text{B.1})$$

so that

$$\mathbf{S}_\alpha^{k_\bullet, l_\bullet} = \mathcal{M}_\alpha^{k_\bullet + l_\bullet} \mathbf{P}_0 + \int_{\mathbf{x} \in \mathbb{R}^d} \chi_\alpha(\mathbf{x}) \mathbf{x}^{k_\bullet} \mathbf{Q}_\alpha^{l_\bullet}(\mathbf{x}) dV_{\mathbf{x}}. \quad (\text{B.2})$$

Assuming inclusion  $\alpha$  is convex, it is possible to perform in Eq. (B.1) the change of variables specified by Eq. (43)

$$\mathbf{Q}_\alpha^{l_\bullet}(\mathbf{x}) = \lim_{\delta \rightarrow 0} \int_{\|\mathbf{n}\|=1} \int_{\delta}^{R_\alpha(\mathbf{x}, \mathbf{n})} (\mathbf{x}_\bullet + r\mathbf{n}_\bullet)^{l_\bullet} \mathbf{Q}_0(r\mathbf{n}) r^{d-1} dr dS_{\mathbf{n}},$$

where  $dS_{\mathbf{n}}$  denotes the surface element at  $\mathbf{n}$  on the unit sphere. From the homogeneity of  $\mathbf{Q}_0$  (see Appendix A)

$$\mathbf{Q}_\alpha^{l_\bullet}(\mathbf{x}) = \lim_{\delta \rightarrow 0} \int_{\|\mathbf{n}\|=1} \left( \int_{\delta}^{R_\alpha(\mathbf{x}, \mathbf{n})} \frac{(\mathbf{x}_\bullet + r\mathbf{n}_\bullet)^{l_\bullet}}{r} dr \right) \mathbf{Q}_0(\mathbf{n}) dS_{\mathbf{n}},$$

where the singularity is removed with the help of the following substitution

$$\frac{(\mathbf{x}_\bullet + r\mathbf{n}_\bullet)^{l_\bullet}}{r} = \frac{(\mathbf{x}_\bullet + r\mathbf{n}_\bullet)^{l_\bullet} - \mathbf{x}_\bullet^{l_\bullet}}{r} + \frac{\mathbf{x}_\bullet^{l_\bullet}}{r}.$$

Indeed, Eq. (1) readily shows that the first term is regular as  $r \rightarrow 0$

$$\frac{(\mathbf{x}_\bullet + r\mathbf{n}_\bullet)^{l_\bullet} - \mathbf{x}_\bullet^{l_\bullet}}{r} = \sum_{\substack{0_\bullet \leq h_\bullet \leq l_\bullet \\ h_\bullet \neq 0_\bullet}} \binom{l_\bullet}{h_\bullet} r^{h_\bullet-1} n_\bullet^{h_\bullet} \mathbf{x}_\bullet^{l_\bullet-h_\bullet},$$

and

$$\begin{aligned} \lim_{\delta \rightarrow 0} \int_{\delta}^{R_\alpha(\mathbf{x}, \mathbf{n})} \frac{(\mathbf{x}_\bullet + r\mathbf{n}_\bullet)^{l_\bullet} - \mathbf{x}_\bullet^{l_\bullet}}{r} dr \\ = \int_0^{R_\alpha(\mathbf{x}, \mathbf{n})} \frac{(\mathbf{x}_\bullet + r\mathbf{n}_\bullet)^{l_\bullet} - \mathbf{x}_\bullet^{l_\bullet}}{r} dr \\ = \sum_{\substack{0_\bullet \leq h_\bullet \leq l_\bullet \\ h_\bullet \neq 0_\bullet}} \binom{l_\bullet}{h_\bullet} \frac{R_\alpha(\mathbf{x}, \mathbf{n})^{h_\bullet}}{h_\bullet} n_\bullet^{h_\bullet} \mathbf{x}_\bullet^{l_\bullet-h_\bullet}. \end{aligned}$$

Therefore,

$$\begin{aligned} \mathbf{Q}_\alpha^{l_\bullet}(\mathbf{x}) &= \int_{\|\mathbf{n}\|=1} \int_0^{R_\alpha(\mathbf{x}, \mathbf{n})} \frac{(\mathbf{x}_\bullet + r\mathbf{n}_\bullet)^{l_\bullet} - \mathbf{x}_\bullet^{l_\bullet}}{r} \mathbf{Q}_0(\mathbf{n}) dr dS_{\mathbf{n}} \\ &+ \mathbf{x}_\bullet^{l_\bullet} \lim_{\delta \rightarrow 0} \int_{\|\mathbf{n}\|=1} \log \frac{R_\alpha(\mathbf{x}, \mathbf{n})}{\delta} \mathbf{Q}_0(\mathbf{n}) dS_{\mathbf{n}}, \end{aligned} \quad (\text{B.3})$$

and, from Eq. (A.6), the integral in the last term reduces to

$$\int_{\|\mathbf{n}\|=1} \log(R_\alpha(\mathbf{x}, \mathbf{n})) \mathbf{Q}_0(\mathbf{n}) dS_{\mathbf{n}}, \quad (\text{B.4})$$

while the change of variables specified by Eq. (43) can be reversed in the first term

$$\int_{\mathbf{y} \in \mathbb{R}^d} \chi_\alpha(\mathbf{y}) (\mathbf{y}^{l_\bullet} - \mathbf{x}_\bullet^{l_\bullet}) \mathbf{Q}_0(\mathbf{y} - \mathbf{x}) dV_{\mathbf{y}}. \quad (\text{B.5})$$

This completes the proof, since Eq. (44) is readily retrieved from Eqs. (B.2), (B.3), (B.4) and (B.5).

### Appendix B.2. Application to spherical inclusions

Let  $a_\alpha$  denote the radius of the spherical inclusion  $\Omega_\alpha$ . It can readily be verified that

$$R_\alpha(\mathbf{x}, \mathbf{n}) = -\mathbf{x} \cdot \mathbf{n} + \sqrt{a_\alpha^2 - \|\mathbf{x}\|^2 + (\mathbf{x} \cdot \mathbf{n})^2}. \quad (\text{B.6})$$

In expanded form, the self-influence pseudotensor of convex inclusions reads [see Eq. (44)]

$$\begin{aligned} \mathbf{S}_\alpha^{k_\bullet, l_\bullet} &= \mathcal{M}_\alpha^{k_\bullet + l_\bullet} \mathbf{P}_0 \\ &+ \sum_{\substack{0_\bullet \leq h_\bullet \leq l_\bullet \\ h_\bullet \neq 0_\bullet}} \binom{l_\bullet}{h_\bullet} \left( \int_{\substack{\mathbf{x} \in \mathbb{R}^d \\ \|\mathbf{n}\|=1}} \chi_\alpha(\mathbf{x}) \frac{R_\alpha(\mathbf{x}, \mathbf{n})^{h_\bullet}}{h_\bullet} \right. \\ &\quad \left. n_\bullet^{h_\bullet} \mathbf{x}_\bullet^{k_\bullet + l_\bullet - h_\bullet} \mathbf{Q}_0(\mathbf{n}) dS_{\mathbf{n}} dV_{\mathbf{x}} \right) \\ &+ \int_{\substack{\mathbf{x} \in \mathbb{R}^d \\ \|\mathbf{n}\|=1}} \chi_\alpha(\mathbf{x}) \log(R_\alpha(\mathbf{x}, \mathbf{n})) \mathbf{x}_\bullet^{k_\bullet + l_\bullet} \mathbf{Q}_0(\mathbf{n}) dS_{\mathbf{n}} dV_{\mathbf{x}}. \end{aligned} \quad (\text{B.7})$$

The third term in Eq. (B.7) vanishes. Indeed, from the identities  $\mathbf{Q}_0(-\mathbf{n}) = \mathbf{Q}_0(\mathbf{n})$  and

$$\int_{\|\mathbf{n}\|=1} f(\mathbf{n}) dS_{\mathbf{n}} = \int_{\|\mathbf{n}\|=1} \frac{f(\mathbf{n}) + f(-\mathbf{n})}{2} dS_{\mathbf{n}}, \quad (\text{B.8})$$

for any function  $f$ , it is found that

$$\begin{aligned} \int_{\|\mathbf{n}\|=1} \log(R_\alpha(\mathbf{x}, \mathbf{n})) \mathbf{Q}_0(\mathbf{n}) dS_{\mathbf{n}} \\ = \int_{\|\mathbf{n}\|=1} \log \sqrt{R_\alpha(\mathbf{x}, -\mathbf{n}) R_\alpha(\mathbf{x}, \mathbf{n})} \mathbf{Q}_0(\mathbf{n}) dS_{\mathbf{n}}. \end{aligned}$$

From Eq. (B.6),  $R_\alpha(\mathbf{x}, -\mathbf{n}) R_\alpha(\mathbf{x}, \mathbf{n}) = a_\alpha^2 - \|\mathbf{x}\|^2$ , and the above integral reduces to

$$\log \sqrt{a_\alpha^2 - \|\mathbf{x}\|^2} \int_{\|\mathbf{n}\|=1} \mathbf{Q}_0(\mathbf{n}) dS_{\mathbf{n}} = \mathbf{0}, \quad (\text{B.9})$$

where Eq. (A.6) has been used. Turning now to the second term of Eq. (B.7), Eq. (B.8) can again be used to transform the integral over the unit sphere

$$\begin{aligned} \int_{\|\mathbf{n}\|=1} R_\alpha(\mathbf{x}, \mathbf{n})^{h_\bullet} n_\bullet^{h_\bullet} \mathbf{Q}_0(\mathbf{n}) dS_{\mathbf{n}} \\ = \int_{\|\mathbf{n}\|=1} \frac{R_\alpha(\mathbf{x}, \mathbf{n})^{h_\bullet} + (-1)^{h_\bullet} R_\alpha(\mathbf{x}, -\mathbf{n})^{h_\bullet}}{2} n_\bullet^{h_\bullet} \mathbf{Q}_0(\mathbf{n}) dS_{\mathbf{n}}. \end{aligned}$$

Using Eq. (B.6), it is readily seen that all odd powers of  $\sqrt{a_\alpha^2 - \|\mathbf{x}\|^2 + (\mathbf{x} \cdot \mathbf{n})^2}$  vanish in the integrand

$$\begin{aligned} \frac{R_\alpha(\mathbf{x}, \mathbf{n})^{h_\bullet} + (-1)^{h_\bullet} R_\alpha(\mathbf{x}, -\mathbf{n})^{h_\bullet}}{2} \\ = (-1)^{h_\bullet} \sum_j \binom{h_\bullet}{2j} (\mathbf{x} \cdot \mathbf{n})^{h_\bullet - 2j} (a_\alpha^2 - \|\mathbf{x}\|^2 + (\mathbf{x} \cdot \mathbf{n})^2)^j. \end{aligned} \quad (\text{B.10})$$

Gathering Eqs. (B.7), (B.9) and (B.10), the following expression of  $\mathbf{S}_\alpha^{k_\bullet l_\bullet}$  is finally found for spherical inclusions

$$\begin{aligned} \mathbf{S}_\alpha^{k_\bullet l_\bullet} &= \mathcal{M}^{k_\bullet+l_\bullet} \mathbf{P}_0 \\ &+ \sum_{\substack{0 \leq h_\bullet \leq l_\bullet \\ h_\bullet \neq 0 \\ 0 \leq 2j \leq h_+}} \frac{(-1)^{h_+}}{h_+} \binom{l_\bullet}{h_\bullet} \binom{h_+}{2j} \left( \int_{\substack{\mathbf{x} \in \mathbb{R}^d \\ \|\mathbf{n}\|=1}} \chi_\alpha(\mathbf{x}) (\mathbf{x} \cdot \mathbf{n})^{h_+-2j} \right. \\ &\left. (a_\alpha^2 - \|\mathbf{x}\|^2 + (\mathbf{x} \cdot \mathbf{n})^2)^j x_\bullet^{k_\bullet+l_\bullet-h_\bullet} n_\bullet^{h_\bullet} \mathbf{Q}_0(\mathbf{n}) dS_{\mathbf{n}} dV_{\mathbf{x}} \right). \end{aligned}$$

The above sum reduces to integrals of trigonometric polynomials. Its computation therefore involves only simple (though tedious) algebra, and can easily be implemented in a computer algebra system.

### Appendix C. Change of basis for the influence pseudotensors

As already argued in Sec. 4, literal expressions of the influence pseudotensors are computed in a convenient, local basis  $(\mathbf{e}'_j)_{1 \leq j \leq d}$ . In order to retrieve the pseudotensors in the global basis  $(\mathbf{e}_i)_{1 \leq i \leq d}$ , a change of basis must be carried out, keeping in mind that the influence pseudotensors are not tensors. This is detailed below.

In the remainder of this section, it will be convenient to introduce the following notation:  $k_{\bullet\bullet}$  denotes doubly indexed tuples of size  $d \times d$ ,  $k_{\bullet\bullet} = (k_{ij})_{1 \leq i, j \leq d}$ . Given  $k_{\bullet\bullet}$ , two  $d$ -tuples are further introduced

$$k_{\bullet+} = (k_{i1} + \dots + k_{id})_{1 \leq i \leq d} \quad \text{and} \quad k_{+\bullet} = (k_{1j} + \dots + k_{dj})_{1 \leq j \leq d},$$

which are the horizontal and vertical projections of  $k_{\bullet\bullet}$ , respectively.

For  $\mathbf{x} \in \mathbb{R}^d$ , let  $x_\bullet$  (resp.  $x'_\bullet$ ) be the coordinates of  $\mathbf{x}$  in the global (resp. local) frame;  $x_\bullet$  is related to  $x'_\bullet$  through the classical formula

$$x_i = R_{ij} x'_j,$$

where  $\mathbf{R}$  is the rotation tensor which maps the global basis onto the local basis ( $\mathbf{e}'_i = \mathbf{R} \cdot \mathbf{e}_i$ ). Then, from the multinomial theorem

$$x_i^p = (R_{ij} x'_j)^p = \sum_{k_+ = p} \frac{p!}{k_1! \dots k_d!} (R_{i1} x'_1)^{k_1} \dots (R_{id} x'_d)^{k_d},$$

and  $x_\bullet^{p_\bullet}$  is expressed as a function of  $x'_\bullet$

$$x_\bullet^{p_\bullet} = \sum_{k_{\bullet+} = p_\bullet} \frac{p_1! \dots p_d!}{k_{11}! \dots k_{dd}!} R^{k_{11}} \dots R^{k_{dd}} x'^{k_{\bullet+}}.$$

Using the above identity, the variables  $x'_\bullet$  and  $y'_\bullet$  are substituted to  $x_\bullet$  and  $y_\bullet$  in Eq. (33)

$$\begin{aligned} \mathbf{T}_{\alpha\beta}^{p_\bullet q_\bullet}(\mathbf{r}) &= \sum_{h_{\bullet+} = p_\bullet} \sum_{k_{\bullet+} = q_\bullet} \frac{p_1! \dots p_d!}{h_{11}! \dots h_{dd}!} \frac{q_1! \dots q_d!}{k_{11}! \dots k_{dd}!} R^{h_{11}+k_{11}} \dots R^{h_{dd}+k_{dd}} \\ &\int_{\mathbf{x}, \mathbf{y} \in \mathbb{R}^d} \chi_\alpha(\mathbf{x}) \chi_\beta(\mathbf{y}) x_\bullet^{h_{\bullet+}} y_\bullet^{k_{\bullet+}} \mathbf{T}_0^\infty(\mathbf{r} + \mathbf{y} - \mathbf{x}) dx'_\times dy'_\times, \end{aligned}$$

where it is recalled that  $\det \mathbf{R} = 1$ . The integrals in the above sums are the influence pseudotensors  $\mathbf{T}_{\alpha\beta}^{h_{\bullet+} k_{\bullet+}}(\mathbf{r})$ , expressed in the local basis

$$\mathbf{T}_{\alpha\beta}^{p_\bullet q_\bullet}(\mathbf{r}) = \int_{\mathbf{x}, \mathbf{y} \in \mathbb{R}^d} \chi_\alpha(\mathbf{x}) \chi_\beta(\mathbf{y}) x_\bullet^{p_\bullet} y_\bullet^{q_\bullet} \mathbf{T}_0^\infty(\mathbf{r} + \mathbf{y} - \mathbf{x}) dx'_\times dy'_\times,$$

which shows that the influence pseudotensors in the global basis can be expressed as a linear combination of the influence pseudotensors in the local basis

$$\mathbf{T}_{\alpha\beta}^{p_\bullet q_\bullet}(\mathbf{r}) = \sum_{r_+ = p_+} \sum_{s_+ = q_+} \Lambda_{r_\bullet s_\bullet}^{p_\bullet q_\bullet} \mathbf{T}_{\alpha\beta}^{r_\bullet s_\bullet},$$

where

$$\Lambda_{r_\bullet s_\bullet}^{p_\bullet q_\bullet} = \sum_{\substack{h_{\bullet+} = p_\bullet \\ h_{\bullet+} = r_\bullet}} \sum_{\substack{k_{\bullet+} = q_\bullet \\ k_{\bullet+} = s_\bullet}} \frac{p_1! \dots p_d!}{h_{11}! \dots h_{dd}!} \frac{q_1! \dots q_d!}{k_{11}! \dots k_{dd}!} R_{11}^{h_{11}+k_{11}} \dots R_{dd}^{h_{dd}+k_{dd}}.$$

Finally, recalling that  $\mathbf{T}_0^\infty$  is a true tensor, and introducing the components  $T_{\alpha\beta,ijkl}^{p_\bullet q_\bullet}(\mathbf{r})$  [resp.  $T_{\alpha\beta,IJKL}^{r_\bullet s_\bullet}(\mathbf{r})$ ] of  $\mathbf{T}_{\alpha\beta}^{p_\bullet q_\bullet}(\mathbf{r})$  [resp.  $\mathbf{T}_{\alpha\beta}^{r_\bullet s_\bullet}(\mathbf{r})$ ] in the global (resp. local) basis, it is found that

$$T_{\alpha\beta,ijkl}^{r_\bullet s_\bullet}(\mathbf{r}) = R_{iI} R_{jJ} R_{kK} R_{lL} \sum_{r_+ = p_+} \sum_{s_+ = q_+} \Lambda_{r_\bullet s_\bullet}^{p_\bullet q_\bullet} T_{\alpha\beta,IJKL}^{r_\bullet s_\bullet}.$$

The above formulas can be used to compute the influence tensor in any basis, provided all influence tensors have been computed in the local basis.

### References

- Benedikt, B., Lewis, M., Rangaswamy, P., 2006. On elastic interactions between spherical inclusions by the equivalent inclusion method. *Computational Materials Science* 37, 380–392.
- Benveniste, Y., 1987. A new approach to the application of Mori-Tanaka's theory in composite materials. *Mechanics of Materials* 6, 147–157.
- Berveiller, M., Fassifehri, O., Hihi, A., 1987. The problem of two plastic and heterogeneous inclusions in an anisotropic medium. *International Journal of Engineering Science* 25, 691–709.
- Brisard, S., Dormieux, L., 2012. Combining Galerkin approximation techniques with the principle of Hashin and Shtrikman to derive a new FFT-based numerical method for the homogenization of composites. *Computer Methods in Applied Mechanics and Engineering* 217–220, 197–212.
- Brisard, S., Dormieux, L., Sab, K., 2013a. Self-influence and influence pseudotensors of  $d$ -dimensional spheres. To be submitted to HAL Open Archive.
- Brisard, S., Sab, K., Dormieux, L., 2013b. New boundary conditions for the computation of the apparent stiffness of statistical volume elements. *Journal of the Mechanics and Physics of Solids* 61, 2638–2658.
- Buryachenko, V.A., 2007. *Micromechanics of Heterogeneous Materials*. Springer.
- Christensen, R.M., Lo, K.H., 1979. Solutions for effective shear properties in three phase sphere and cylinder models. *Journal of the Mechanics and Physics of Solids* 27, 315–330.
- Coenen, E.W.C., Kouznetsova, V.G., Geers, M.G.D., 2012. Novel boundary conditions for strain localization analyses in microstructural volume elements. *International Journal for Numerical Methods in Engineering* 90, 1–21.
- El Mouden, M., Molinari, A., 2000. Thermoelastic properties of composites containing ellipsoidal inhomogeneities. *Journal of Thermal Stresses* 23, 233–255.
- Ern, A., Guermond, J.L., 2004. *Theory and Practice of Finite Elements*. volume 159 of *Applied Mathematical Sciences*. Springer.
- Eshelby, J.D., 1957. The determination of the elastic field of an ellipsoidal inclusion, and related problems. *Proceedings of the Royal Society of London. Series A, Mathematical and Physical Sciences* 241, 376–396.

- Fond, C., Géhant, S., Schirrer, R., 2002. Effects of mechanical interactions on the hydrostatic stress in randomly distributed rubber particles in an amorphous polymer matrix. *Polymer* 43, 909–919.
- Fond, C., Riccardi, A., Schirrer, R., Montheillet, F., 2001. Mechanical interaction between spherical inhomogeneities: an assessment of a method based on the equivalent inclusion. *European Journal of Mechanics - A/Solids* 20, 59–75.
- Gusev, A.A., 1997. Representative volume element size for elastic composites: A numerical study. *Journal of the Mechanics and Physics of Solids* 45, 1449–1459.
- Hashin, Z., Shtrikman, S., 1962a. On some variational principles in anisotropic and nonhomogeneous elasticity. *Journal of the Mechanics and Physics of Solids* 10, 335–342.
- Hashin, Z., Shtrikman, S., 1962b. A variational approach to the theory of the elastic behaviour of polycrystals. *Journal of the Mechanics and Physics of Solids* 10, 343–352.
- Hazanov, S., Huet, C., 1994. Order relationships for boundary conditions effect in heterogeneous bodies smaller than the representative volume. *Journal of the Mechanics and Physics of Solids* 42, 1995–2011.
- Hervé, E., Zaoui, A., 1993. n-layered inclusion-based micromechanical modelling. *International Journal of Engineering Science* 31, 1–10.
- Hill, R., 1963a. Elastic properties of reinforced solids: Some theoretical principles. *Journal of the Mechanics and Physics of Solids* 11, 357–372.
- Hill, R., 1963b. New derivations of some elastic extremum principles, in: *Progress in Applied Mechanics – The Prager 60th Anniversary Volume*. Macmillan, New York, pp. 99–106.
- Hill, R., 1967. The essential structure of constitutive laws for metal composites and polycrystals. *Journal of the Mechanics and Physics of Solids* 15, 79–95.
- Kanaun, S.K., Levin, V.M., 2008. *Self-Consistent Methods for Composites Vol.1: Static Problems*. volume 148 of *Solid Mechanics and its Applications*. Springer.
- Kanit, T., Forest, S., Galliet, I., Mounoury, V., Jeulin, D., 2003. Determination of the size of the representative volume element for random composites: statistical and numerical approach. *International Journal of Solids and Structures* 40, 3647–3679.
- Korringa, J., 1973. Theory of elastic constants of heterogeneous media. *Journal of Mathematical Physics* 14, 509–513.
- Kröner, E., 1974. On the physics and mathematics of self-stresses, in: Zeman, J.L., Ziegler, F. (Eds.), *Topics in Applied Continuum Mechanics*, Springer Verlag Wien, pp. 22–38.
- Kröner, E., 1977. Bounds for effective elastic moduli of disordered materials. *Journal of the Mechanics and Physics of Solids* 25, 137–155.
- Mandel, J., 1972. *Plasticité classique et viscoplasticité*. Number 97 in CISM courses and lectures, Springer.
- Molinari, A., El Mouden, M., 1996. The problem of elastic inclusions at finite concentration. *International Journal of Solids and Structures* 33, 3131–3150.
- Mori, T., Tanaka, K., 1973. Average stress in matrix and average elastic energy of materials with misfitting inclusions. *Acta Metallurgica* 21, 571–574.
- Moschovidis, Z.A., Mura, T., 1975. Two-ellipsoidal inhomogeneities by the equivalent inclusion method. *Journal of Applied Mechanics* 42, 847–852.
- Moulinec, H., Suquet, P., 1998. A numerical method for computing the overall response of nonlinear composites with complex microstructure. *Computer Methods in Applied Mechanics and Engineering* 157, 69–94.
- Mura, T., 1987. *Micromechanics of defects in solids*. Martinus Nijhoff Publishers. 2 edition.
- Nakasone, Y., Nishiyama, H., Nojiri, T., 2000. Numerical equivalent inclusion method: a new computational method for analyzing stress fields in and around inclusions of various shapes. *Materials Science and Engineering: A* 285, 229–238.
- Novák, J., Kaczmarczyk, L., Grassl, P., Zeman, J., Pearce, C.J., 2012. A micromechanics-enhanced finite element formulation for modelling heterogeneous materials. *Computer Methods in Applied Mechanics and Engineering* 201-204, 53–64.
- Ostoja-Starzewski, M., 2006. Material spatial randomness: From statistical to representative volume element. *Probabilistic Engineering Mechanics* 21, 112–132.
- Rodin, G.J., 1993. The overall elastic response of materials containing spherical inhomogeneities. *International Journal of Solids and Structures* 30, 1849–1863.
- Rodin, G.J., Hwang, Y.L., 1991. On the problem of linear elasticity for an infinite region containing a finite number of non-intersecting spherical inhomogeneities. *International Journal of Solids and Structures* 27, 145–159.
- Sab, K., 1992. On the homogenization and the simulation of random materials. *European Journal of Mechanics - A/Solids* 11, 585–607.
- Salmi, M., Auslender, F., Bornert, M., Fogli, M., 2012. Apparent and effective mechanical properties of linear matrix-inclusion random composites: Improved bounds for the effective behavior. *International Journal of Solids and Structures* 49, 1195–1211.
- Shodja, H.M., Rad, I.Z., Soheilifard, R., 2003. Interacting cracks and ellipsoidal inhomogeneities by the equivalent inclusion method. *Journal of the Mechanics and Physics of Solids* 51, 945–960.
- Suquet, P. (Ed.), 1997. *Continuum Micromechanics*. Number 377 in CISM courses and lectures, SpringerWienNewYork.
- Szabó, B., Düster, A., Rank, E., 2004. The *p*-version of the finite element method, in: Stein, E., De Borst, R., Hugues, T.J.R. (Eds.), *Encyclopedia of Computational Mechanics*. John Wiley & Sons, Ltd. chapter 5, pp. 119–139.
- Torquato, S., 2002. *Random heterogeneous materials: microstructure and macroscopic properties*. Springer-Verlag.
- Walpole, L.J., 1969. On the overall elastic moduli of composite materials. *Journal of the Mechanics and Physics of Solids* 17, 235–251.
- Willis, J.R., 1977. Bounds and self-consistent estimates for the overall properties of anisotropic composites. *Journal of the Mechanics and Physics of Solids* 25, 185–202.
- Zeller, R., Dederichs, P.H., 1973. Elastic constants of polycrystals. *Physica Status Solidi (B)* 55, 831–842.